Journal of Cell Science 108, 3013-3028 (1995)
Printed in Great Britain © The Company of Biologists Limited 1995

Monoclonal and polyclonal antibodies detect a new type of post-translational modification of axonemal tubulin

Nicolette Levilliers[1,*], Anne Fleury[1] and Anne-Marie Hill[2]

[1]Laboratoire de Biologie Cellulaire 4, URA 1134 CNRS, Bâtiment 444, Université de Paris-Sud, 91405 Orsay Cedex, France
[2]Laboratoire de Physiologie et Pharmacologie Cellulaire, U 274 INSERM, Bâtiment 443, Université de Paris-Sud, 91405 Orsay Cedex, France

*Author for correspondence

SUMMARY

Polyclonal (PAT) and monoclonal (AXO 49) antibodies against *Paramecium* axonemal tubulin were used as probes to reveal tubulin heterogeneity. The location, the nature and the subcellular distribution of the epitopes recognized by these antibodies were, respectively, determined by means of: (i) immunoblotting on peptide maps of *Paramecium*, sea urchin and quail axonemal tubulins; (ii) immunoblotting on ciliate tubulin fusion peptides generated in *E. coli* to discriminate antibodies directed against sequential epitopes (reactive) from post-translational ones (non reactive); and (iii) immunofluorescence on *Paramecium* cells, using throughout an array of antibodies directed against tubulin sequences and post-translational modifications as references.

AXO 49 monoclonal antibody and PAT serum were both shown to recognize epitopes located near the carboxyl-terminal end of both subunits of *Paramecium* axonemal tubulin, whereas the latter recognized additional epitopes in α-tubulin; AXO 49 and a fraction of the PAT serum proved to be unreactive over fusion proteins; both PAT and AXO 49 labelled a restricted population of very stable microtubules in *Paramecium*, consisting of axonemal and cortical ones, and their reactivity was sequentially detected following microtubule assembly; finally, both antibodies stained two upward spread bands in *Paramecium* axonemal tubulin separated by SDS-PAGE, indicating the recognition of various α- and β-tubulin isoforms displaying different apparent molecular masses.

These data, taken as a whole, definitely establish that PAT and AXO 49 recognize a post-translational modification occurring in axonemal microtubules of protozoa as of metazoa. This modification appears to be distinct from the previously known ones, and all the presently available evidence indicates that it corresponds to the very recently discovered polyglycylation of *Paramecium* axonemal α- and β-tubulin.

Key words: axonemal tubulin, stable microtubule, *Paramecium*, anti-tubulin antibody, peptide mapping, post-translational modification, acetylation, polyglutamylation, polyglycylation

INTRODUCTION

Structural and functional diversity is commonly observed among the microtubular networks in eukaryotic cells. This diversity can be generated from the structure and localization of the microtubule-organizing centers (MTOCs), through interactions between microtubules (MTs) and microtubule-associated proteins (MAPs), and from the heterogeneity of MTs at a molecular level. At the cellular level, different isotypes of α- and β-tubulins are found which are encoded by multigenic families and the number of tubulin genes increases from unicellular to multicellular eukaryotes (Raff, 1984; Cleveland and Sullivan, 1985; Little and Seehaus, 1988; Sullivan, 1988; Silflow, 1991; Gaertig et al., 1993; Luduena, 1993). However, the great variety of isoforms is generated by combinations of numerous post-translational modifications (PTMs) occurring on relatively few primary gene products (McKeithan et al., 1983; Suprenant et al., 1985; Denoulet et al., 1988; Eddé et al., 1991; Fouquet et al., 1994). As concerns α-tubulin, acetylation of Lys 40 (L'Hernault and Rosenbaum, 1985; LeDizet and Piperno, 1987; Eddé et al., 1991), polyglutamylation of Glu 445 (Eddé et al., 1990), and at the C-terminal end, detyrosination (Barra et al., 1974; Thompson, 1982) and removal of a glutamyl-tyrosine dipeptide (Paturle-Lafanechère et al., 1991) have been reported. As for β-tubulin, phosphorylation of Tyr 437 and Ser 444 in the βIII isotype and of Ser 441 in the βVI isotype (Eipper, 1974; Luduena et al., 1988; Diaz-Nido et al., 1990; Alexander et al., 1991; Rüdiger and Weber, 1993), and glutamylation of glutamate residues (Glu 434, 435, 438 or 441) differing according to the isotype (Alexander et al., 1991; Redeker et al., 1992; Rüdiger et al., 1992; Mary et al., 1994) have been described. Among these modifications, all demonstrated in metazoa, only acetylation has been thoroughly characterized in a protist.

The study of the relation between MT diversity and tubulin heterogeneity has been approached here through the use of immunological tools in a ciliate protist, *Paramecium*. Such a model combines a higher MT diversity than a single metazoan

cell with a more reduced genetic diversity. Thus, the 13 microtubular arrays displaying different stability and immunological properties identified in this unicellular organism (Cohen and Beisson, 1988; Torres and Delgado, 1989; Adoutte et al., 1991; Fleury et al., 1995) appear to be built from few types of tubulin molecules: all the gene sequence data available indicate that the resulting proteins are extremely similar (Dupuis, 1992a,b). Therefore, in this protist, tubulin heterogeneity is expected to be mostly, if not exclusively, generated through PTMs, and the present study illustrates this statement.

Previous work had shown that a serum raised against *Paramecium* axonemal tubulin (later named anti-PA tubulin antibody then PAT) reacts specifically with axonemal and cortical MTs of *Paramecium* (Cohen et al., 1982) and other protists (Brugerolle and Adoutte, 1988), and also with axonemal tubulins from a broad range of species, extending from protists to mammals, whereas it is unreactive with cytoplasmic tubulins of metazoa (Adoutte et al., 1985). Taking into account the fact that most stable, long-lived MTs are post-translationally modified (Sullivan, 1988; Greer and Rosenbaum, 1989, for reviews), the PAT immunoreactivity restricted to a subset of stable MTs in *Paramecium* and its late occurrence in the course of cell division provided the first arguments permetting to hypothesize that the serum would recognize a post-translational modification taking place on previously assembled MTs (Adoutte et al., 1991).

In order to identify the major epitope recognized by the PAT serum, we recently produced monoclonal antibodies (mAbs), using *Paramecium* axonemes as antigen, and one of them, AXO 49, appeared to exhibit immunocytochemical properties similar to those of the serum (Callen et al., 1994).

Therefore we have undertaken an exhaustive comparison of the location, the nature and the subcellular distribution of the epitopes recognized by both polyclonal and monoclonal antibodies, by means of: (i) immunoblotting on peptide maps of *Paramecium* axonemal tubulin; (ii) immunoblotting over fusion proteins expressed in *E. coli*, a procedure which can discriminate antibodies that are directed against sequential epitopes (reactive ones), from those directed against post-translational epitopes (non reactive); or (iii) single and double labelling immunofluorescence of *Paramecium* cells, the latter method permitting to compare kinetics of appearance of the respective epitopes in newly assembled MTs. AXO 49 and PAT turned out to be both directed to a post-translational modification of tubulin, located in the extreme C-terminal part of both subunits and distinct from previously known ones detected by reference mAbs. These data have led us to search for a new modification of *Paramecium* axonemal tubulin. In a separate work, C-terminal peptides have been subjected to physico-chemical analysis and have been shown to carry a new post-translational modification, consisting of the addition of glycyl units to the γ carboxyl groups of Glu 445 and Glu 437 of the α and β subunits, respectively, and termed polyglycylation (Redeker et al., 1994). The characteristics of the PTM recognized by both antibodies described here fit very well with those of the polyglycylation. In addition, they provide the first clues suggesting the occurrence of different forms of polyglycylation in a cell. Finally, we have shown that this previously undescribed PTM occurs in axonemal tubulins from very distant species in the evolutionary scale, ranging from *Paramecium* to sea urchin and quail.

MATERIALS AND METHODS

Cells

Paramecium tetraurelia cells (strain d4-2) were grown as reported by Callen et al. (1994).

Protein preparations

Paramecium axonemes and axonemal tubulin were prepared as previously described (Geuens et al., 1989).

Quail oviduct ciliary axonemes were prepared by M. C. Marty (CNRS, Ivry-sur-Seine, France), as described by Adoutte et al. (1991).

Sea urchin *(Paracentrotus lividus)* spermatozoan flagellar axonemes (provided by M. P. Cosson, CNRS, Villefranche-sur-Mer, France) were prepared according to the method of Gibbons and Fronk (1972).

Fusion proteins were prepared as detailed by Callen et al. (1994). Briefly, the plasmids encoding β-galactosidase/α-tubulin fusion proteins were constructed as follows. DNA of one α-tubulin gene from *Stylonychia lemnae* (Helftenbein and Müller, 1988) cloned in pBR322 (a kind gift from F. Caron, Ecole Normale Supérieure, Paris) was digested with various restriction endonucleases. The gene fragments were then inserted in the pEX vectors (Boehringer, Mannheim, Germany) downstream from the *lacZ* gene under control of a λ promoter. The expressed inserts correspond to the 5 following domains of α-tubulin lying at positions 22-176, 214-445, 274-338, 339-445 and 412-445 (Fig. 4). The protein domain 177-213 cannot be expressed because of the presence of an universal STOP codon UAA encoding glutamine (position 177) in the α-tubulin gene of *Stylonychia*, and of the absence of a suitable restriction endonuclease site upstream of position 214.

Anti-tubulin antibodies

Reference antibodies

Polyclonals

Affinity-purified C85, C105 and C140 monospecific antibodies (Arévalo et al., 1990) were generously provided by Dr J. M. Andreu (Centro de Investigaciones Biologicas, Madrid, Spain).

Monoclonals

DM1A and DM1B mAbs (Blose et al., 1984) were purchased from Amersham (Les Ulis, France); 6-11B-1 cell culture supernatant (Piperno and Fuller, 1985) was a generous gift from Dr G. Piperno (Mount Sinai Medical School, New York, USA) whereas ascites fluid was purchased from Sigma (Saint-Quentin-Favallier, France); TU-01 (Viklicky et al., 1982) was kindly provided by Dr V. Viklicky (Czechoslovak Academy of Sciences, Prague, Czech Republic) and GT335 (Wolff et al., 1992) was generously given by Dr A. Wolff (Collège de France, Paris).

Preparation of anti-axonemal tubulin antibodies

The serum (4th sample taken in the course of rabbit immunization) raised against *Paramecium* axonemal tubulin in acrylamide (Cohen et al., 1982) was employed crude (PAT) or affinity-purified using *Paramecium* axonemal tubulin, as previously described (Geuens et al., 1989). Two peaks, PAT 1 and PAT 2, were, respectively, eluted at pH 2.8 and 2.2.

AXO 49 mAb was prepared as described by Callen et al. (1994), and used as cell culture supernatant or (when mentioned) affinity-purified by means of Affi-Prep protein A MAPS II kit from Bio-Rad (Ivry-sur-Seine, France).

Limited proteolysis

Proteolysis of soluble *Paramecium* axonemal tubulin, 0.5-4 mg/ml in MES buffer at pH 6.8 (50 mM MES, 1 mM EGTA, 1 mM $MgCl_2$, 1 mM GTP) was performed by incubation for 30 minutes at 30°C with the following proteases at the indicated weight ratios: trypsin, 1.2%;

pronase, 0.2%; subtilisin B (Novo, Copenhagen, Denmark), 2%. The reaction was stopped by addition of 2 mM PMSF.

Gel electrophoresis, immunoblotting and dot-blotting

SDS-PAGE was conducted according to the method of Laemmli (1970), using 0.75 mm thick, 12 cm long, 8% polyacrylamide gels or (when mentioned) 10% polyacrylamide mini-gels at pH 8.3, with 0.1% (w/v) SDS (99% pure) from BDH Laboratory Supplies (Poole, England). Gels were stained with Coomassie Blue or electro-transferred according to Kyhse-Andersen (1984), and membranes were processed as described previously (Callen et al., 1994). Dot-blot analysis of peptides was performed after covalent binding to Immobilon-AV affinity membrane (Millipore, Saint-Quentin en Yvelines, France), according to Canas et al. (1993). Peroxidase-labelled secondary antibodies (sheep anti-mouse or goat anti-rabbit IgGs from Diagnostics Pasteur, Marnes-la-Coquette, France) were used at 1:2,000 and peroxidase was detected using enhanced chemiluminescence (ECL, Amersham).

Peptide mapping

For in-gel digestion, α- and β-tubulin bands were separated then cut out from 0.75 mm thick, 12 cm long, 7.5-15% or 8% SDS-polyacrylamide gels performed either at pH 8.25 to get an optimal separation of *Paramecium* tubulin subunits, or at pH 9.25 to separate sea urchin and quail tubulin subunits. Under these respective conditions, *Paramecium* α-tubulin migrates faster than β-tubulin, whereas the relative migrations of both subunits of metazoan tubulins are reversed (Suprenant et al., 1985). Then the *Paramecium* and metazoan tubulin bands were loaded onto 1 mm thick, 11 cm long SDS-polyacrylamide gels made of 15-20% acrylamide gradients at pH 8.25 and 9.25, respectively.

The bands were submitted to proteolysis either by formic acid, according to Sonderegger et al. (1982), or by *Staphylococcus aureus* V8 protease (type XVII-B, Sigma), after Cleveland et al. (1977). The latter procedure is detailed by Callen et al. (1994). Briefly, gels were either silver-stained according to the method of Merril et al. (1981, 1983), or electro-transferred according to Towbin et al. (1979). After overnight incubation with primary antibodies, the filters were successively incubated with biotinylated secondary antibodies (goat anti-mouse or donkey anti-rabbit IgG at 1:1,600), then with streptavidin-biotinylated horseradish peroxidase complex at 1:1,600 (Amersham), and detection was carried out using ECL. In one case, detection was performed using peroxidase or alkaline phosphatase-labelled secondary antibodies and DAB or NBT/BCIP, respectively, as previously described (Adoutte et al., 1991).

Immunofluorescence microscopy

The immunocytochemical procedure is reported by Callen et al. (1994). Fluorescein-labelled sheep anti-mouse and goat anti-rabbit IgGs at 1:200 (Diagnostics Pasteur) and Texas Red-conjugated goat anti-rabbit IgG at 1:50 (Jackson Immunoresearch Laboratories, West Grove, PA, USA) were used as secondary antibodies. Cells were examined on a Bio-Rad Lasersharp MRC 600 confocal microscope with an argon laser for single staining and a two-laser equipment (argon and helium-neon) for double staining.

RESULTS

AXO 49 mAb and PAT serum recognize epitopes located in a broad C-terminal domain of *Paramecium* axonemal α- and β-tubulin

Following in-gel digestion of *Paramecium* axonemal α- and β-tubulins by V8 protease (see below, Fig. 7, lanes a-c, and Fig. 5 in Callen et al., 1994), immunoblotting was achieved with AXO 49 mAb and PAT serum (Fig. 1). Both antibodies react more strongly at the level of the β subunit than of the α one (lanes e,f,m,n). After digestion, AXO 49 reacts only with one β peptide, of 21 kDa (lanes c,d) and one α peptide, of 19 kDa (lanes g,h). PAT stains the same peptides as AXO 49 (lanes k,l,o,p), but relatively more strongly the α ones (lanes g,h,o,p), suggesting the recognition of several epitopes in this domain. These α and β peptides are also, respectively, labelled by DM1A and DM1B (Fig. 1, lanes r,s, and Fig. 7, lanes e,f and h,i) which react with C-terminal (Ct) epitopes of α- and β-tubulin, respectively (Breitling and Little, 1986; and Fig. 4). Therefore the α 19 kDa and β 21 kDa peptides are situated in the C-terminal domain of each subunit. PAT additionally stains 34 and 30 kDa peptides arising from digestion of α-tubulin (Fig. 1, lanes o-r) also labelled by 6-11B-1 (lane t), directed to acetylated Lys 40 of α-tubulin (LeDizet and Piperno, 1987; and Fig. 4); these peptides are therefore comprised in the N-terminal (Nt) domain of α-tubulin.

Paramecium axonemal tubulin was also cleaved in solution by pronase and formic acid which generated α and β 36 and 18 kDa peptides, whereas α-tubulin only was digested by trypsin (not shown). PAT mostly labelled the smaller α and β Ct domains, stained by DM1A and DM1B, respectively, and less strongly the larger α Nt ones labelled by 6-11B-1 (not shown).

The proteolysis patterns of *Paramecium* tubulin are in agreement with those obtained with brain tubulin by Brown and Erickson (1983), Mandelkow et al. (1985), Serrano et al. (1986) and de la Vina et al. (1988). The peptide locations deduced here from antibody immunoreactivity fit with those determined in brain tubulin by sequencing (Mandelkow et al., 1985). The formic acid main cleavage sites were located at peptide bonds Asp 306-Pro 307 in both subunits of porcine brain tubulin (Serrano et al., 1984b); from the conservation of these residues in tubulin from brain (Krauhs et al., 1981) with respect to *Paramecium* (Dupuis, 1992a,b), identical formic acid cleavage sites can be inferred in *Paramecium* tubulin, yielding large Nt and smaller Ct fragments, as actually found.

In conclusion, AXO 49 and PAT recognize epitopes located in a broad C-terminal domain of each subunit (covering 1/3 of the molecules) of *Paramecium* axonemal tubulin, whereas PAT recognizes (an) additional epitope(s) lying in a larger N-terminal domain (2/3 of the molecule) of the α subunit (see Fig. 4).

AXO 49 and PAT react with extreme C-terminal epitopes of *Paramecium* axonemal α- and β-tubulin

AXO 49 and PAT stain two upward spread bands in *Paramecium* axonemal tubulin at the level of both subunits, but the staining of α-tubulin by AXO 49 is slightly shifted upwards relative to that provided by DM1A (Fig. 2, lanes a-d).

Limited proteolysis of axonemal tubulin with subtilisin generates two polypeptides, α_s and β_s, displaying electrophoretic mobilities greater than those of the α and β subunits (CB, lanes e,f), indicating the removal of small fragments, as for brain tubulin (Serrano et al., 1984a). The spread staining of the whole subunits with Coomassie Blue (lane e) as well as with DM1A and DM1B mAbs (lanes a,c) contrasts with the distinct staining of the α_s and β_s polypeptides (lanes f,g,i); the lack of labelling at the level of the uncleaved subunits shows that the proteolysis was complete. AXO 49 is completely unre-

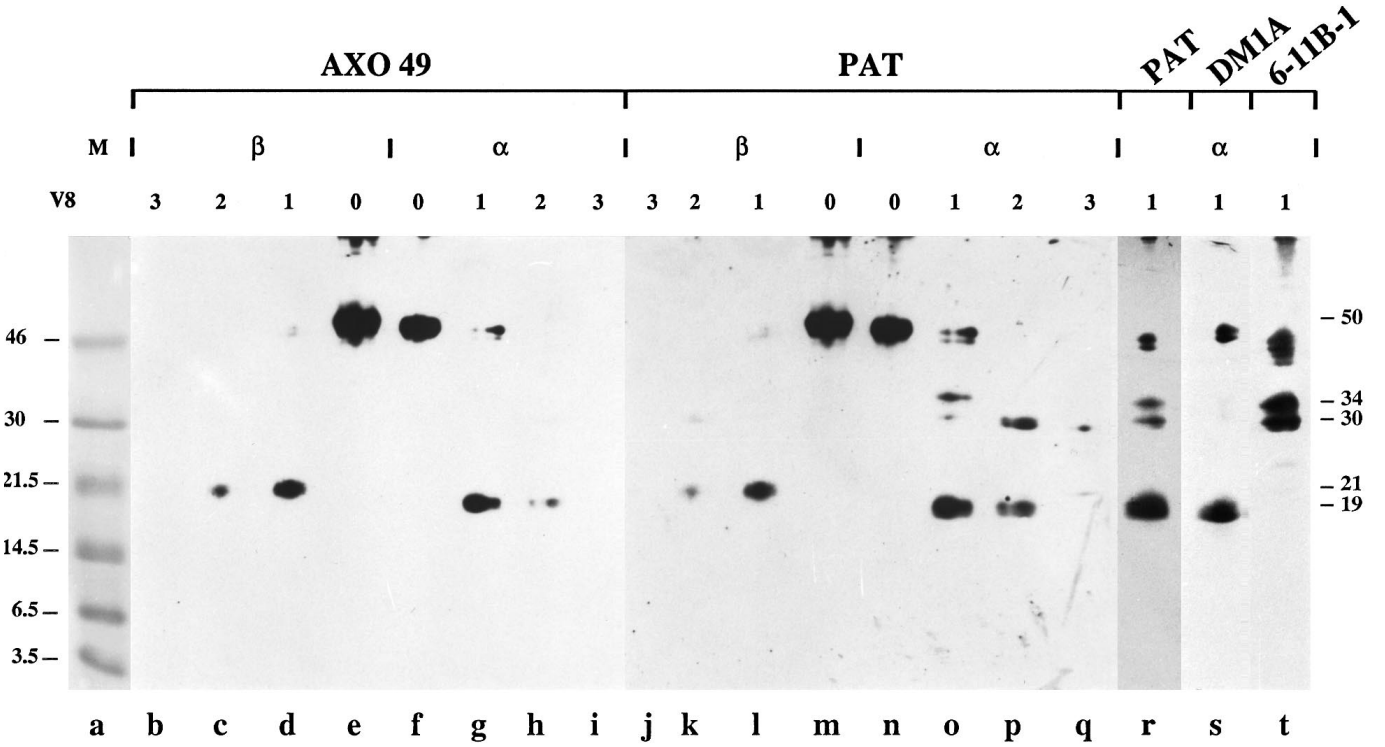

Fig. 1. Immunoblotting of V8 protease peptide maps of *Paramecium* axonemal α- and β-tubulins with AXO 49 mAb and PAT serum. Lane a (M), Rainbow markers with their molecular masses (in kDa) indicated on the left. Lanes e,m and f,n, 2.5 μg of undigested β- and α-tubulins, respectively (assuming that tubulin represents 50% of the axoneme protein amount), denoted 0 in the upper line entitled 'V8'. In the other lanes, 3.75 μg of β- or α-tubulin digested with 0.002, 0.02 or 0.2 μg V8 protease, respectively, named 1, 2, 3 in the upper line 'V8'. Lanes b-i were incubated with purified AXO 49 mAb (25 μg/ml) then with PAT serum at $1:5\times10^3$ (lanes j-q); detection was carried out using ECL. Lanes r,s,t were, respectively, incubated with PAT (1:800), DM1A ($1:10^3$) and 6-11B-1 cell culture supernatant (1:40); detection was achieved with DAB (r) and NBT/BCIP (s,t), and given its lower sensitivity than ECL, it necessitated higher antibody concentrations but gave similar results. The apparent molecular masses of the immunoreactive polypeptides, determined from their migrations (see Callen et al., 1994) are indicated on the right. AXO 49 mAb and PAT serum react with the same Ct β 21 (c,d,k,l) and α 19 kDa peptides (g,h,o,p). The amount of β 21 kDa peptide, revealed by silver staining, being far lower than that of the α 19 kDa peptide (see Fig. 7, lanes b,c), the equivalent labelling of both peptides indicates that both antibodies react more strongly with the β peptide. PAT recognizes additional Nt 34, 30 and 21 kDa peptides (o-q); the latter one, occurring at a high protease concentration (q) and hardly visible here, is best detected at longer exposure times. The same peptides are stained after single (r) or double labelling (o).

active with the α_s and β_s polypeptides (lane h) while still reactive with the whole set of digestion products (see inset). Consequently, the epitopes recognized by AXO 49 were not merely destroyed by cleavage and are born by the small peptides separated after electrophoresis. PAT fairly reacts with α_s but hardly with β_s (lane j), indicating the presence of (an) additional reactive epitope(s) born by the α_s (and β_s) polypeptide(s).

In order to locate the sites of subtilisin cleavage in *Paramecium* tubulin and the epitopes recognized by AXO 49 mAb and PAT serum, V8 protease peptide maps of the whole and subtilisin-digested subunits, α_s and β_s, were compared. C85 and C105 antibodies, which are directed to epitopes located near the C-terminal end of α- and β-tubulin, respectively (Arévalo et al., 1990; and Fig. 4), label α_s 18 and β_s 19 kDa peptides, downward shifted relative to the α 19 and β 21 kDa ones (Fig. 3, lanes b,e,f,i). As expected, AXO 49 is unreactive towards the former peptides (lanes d,g) while strongly reactive with the latter ones (lanes c,h). Unlike AXO 49, PAT still reacts moderately with the α_s 18 kDa peptide (lanes c,d,k,l) but hardly with the β_s 19 kDa one (lanes g,h,n,o). In contrast, neither the migration rates nor the reactivities of the α 34 and 30 kDa peptides with 6-11B-1 and PAT are affected by subtilisin digestion (lanes j-m). Remarkably, one purified fraction from the serum, PAT 1, displays a very weak reactivity with the α_s 18 and β_s 19 kDa peptides (lanes p-s), suggesting that it is enriched in an antibody similar to the AXO 49 mAb. In contrast, the reactivity pattern of the second fraction, PAT 2 (lanes t-w), is very similar to that of the whole serum.

Thus, double proteolysis, yielding unmodified Nt peptides and smaller Ct ones than with V8 protease only, demonstrates that subtilisin cleaves, in *Paramecium*, as in brain tubulin (Serrano et al., 1984a,b), both subunits near their C-terminal ends. The loss of AXO 49 mAb reactivity towards subtilisin-cleaved *Paramecium* axonemal tubulin, and the conservation of the epitopes recognized by DM1A and DM1B (Fig. 2) and C85 and C105 antibodies (Fig. 3) permitted us to localize: (i) the subtilisin cleavage sites approximately downstream of the most rightward of these epitopes, i.e. probably on the Ct side of residues 443 and 431 of the α and β subunits, respectively,

namely 6 to 11 residues from their Ct extremities; (ii) the epitopes recognized by AXO 49 downstream of the subtilisin cleavage sites, therefore in the extreme C-terminal part of both subunits, probably in the respective sequence segments 444-449 and 432-442 of α- and β-tubulin. In addition, the important decrease of PAT serum reactivity in single (Fig. 2) and double (Fig. 3) proteolysis experiments shows that the latter recognizes several epitopes: (i) mainly the same ones as those reacting with AXO 49 mAb, located near the C-terminal end of both subunits; (ii) epitopes lying upstream of the previous ones, i.e. in broad C-terminal domains of both subunits delimited at their Nt sides, by the position of the α_s 18 and β_s 19 kDa peptides, starting at residues 267 and 257, respectively, and at their Ct ends, by the subtilisin cleavage sites; (iii) an epitope located in a broad N-terminal region of the α subunit (1-213), delimited by the smallest reactive Nt peptide, of 21 kDa (Fig. 1, lane q). The positions of the epitopes recognized by AXO 49 and PAT are represented in Fig. 4.

The locations of the Ct epitopes rely upon determinations of the subtilisin cleavage sites, inferred from reactivities of site-directed antibodies. For α-tubulin, the epitope was restricted to a small segment, thanks to the availability of an antibody directed to a very Ct sequential epitope (C85). However, the accuracy of such determinations is limited by the lack of information on the minimal sequences compatible with immunoreactivity. In fact, two conflicting views have been reported for

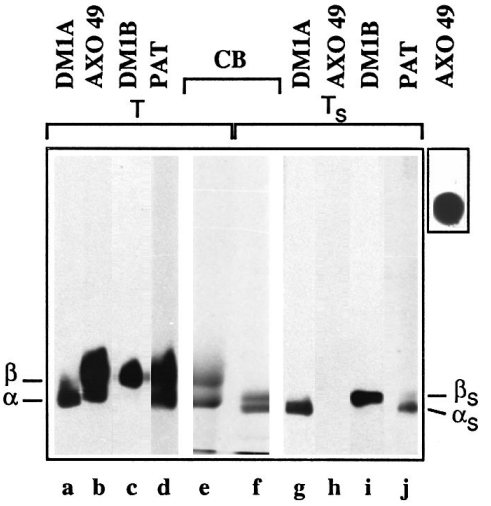

Fig. 2. Immunoblotting analysis of *Paramecium* axonemal tubulin before (T) and after proteolysis with subtilisin (T_S). The mobilities of the subtilisin-digested subunits (α_s, β_s) are greater than those of the uncleaved subunits (α, β). Protein amounts: CB, Coomassie Blue staining, 6 μg T and 7.5 μg T_s (lanes e and f); immunoblotting, 0.4 μg T and 0.5 μg T_s/well (lanes a-d and g-j). Antibody dilutions: DM1A, $1:10^4$ (a,g); AXO 49, 1:10 (b,h); DM1B, $1:4\times10^4$ (c,i) ; PAT, $1:2\times10^4$ (d,j). Note that lanes a and b, g and h are paired half-tracks which permit us to ascertain: (1) the upward shift of AXO 49 reactivity with T with respect to that of DM1A; (2) the lack of reactivity of AXO 49 with T_s in comparison with the strong reactivity of DM1A. Long exposure times were used for ECL detection in order to visualize the spread staining of the tubulin subunits with DM1A and DM1B (a,c) contrasting with the sharp staining of the α_s and β_s polypeptides (g,i); and to yield a strong staining of tubulin with AXO 49 and PAT (b,d) permitting us to ascertain the respective total lack and very weak residual reactivity of both antibodies with α_s and β_s polypeptides (h,j). Inset, dot-blot analysis of subtilisin-digested *Paramecium* tubulin (1 μg) with AXO 49 (1:50). The specificity of the AXO 49 reaction with the digestion products (inset, lower square) is demonstrated by comparison with the lack of reaction of AXO 49 with 2 μg of an unrelated protein, ovomucoid trypsin inhibitor (upper square).

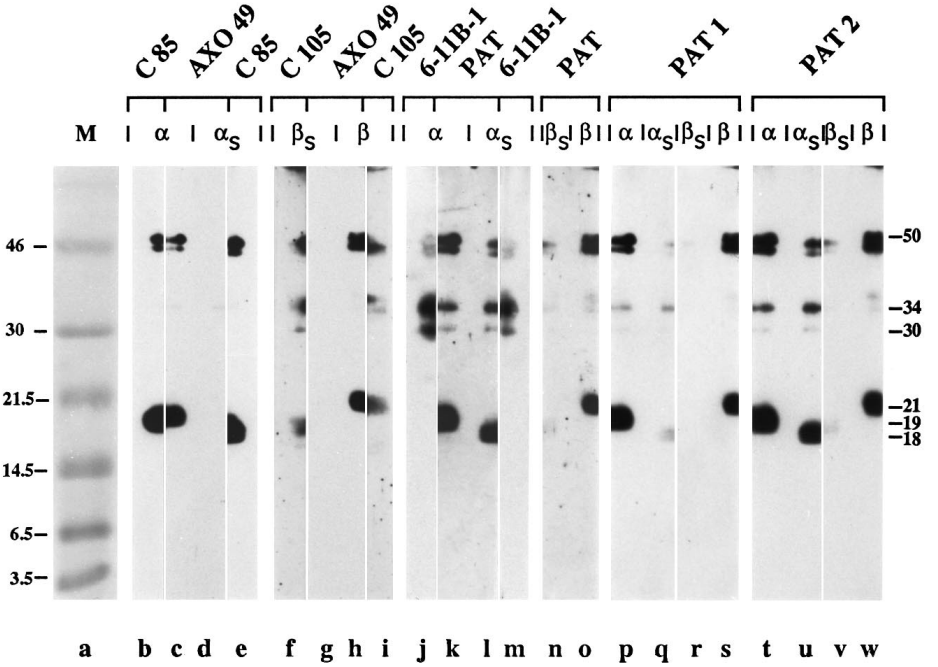

Fig. 3. Comparative immunoblotting analysis of V8 protease peptide maps of whole (α, β) and subtilisin-digested (α_s, β_s) *Paramecium* axonemal tubulin subunits. Lane a (M), Rainbow markers with their molecular masses (in kDa). In the other wells, either 3 μg of α- or β-tubulin, or 5.5 μg of α_s or β_s polypeptide, cut out from gels, were digested with 0.002 μg V8 protease. Each track was divided in 2 halves after transfer, so that contiguous lanes from b to m represent paired half-tracks, which permits us to ensure a convincing comparison of the peptide mobilities and reactivities with different antibodies. Antibody dilutions: C85, 0.3 μg/ml (b,e); AXO 49, 1:10, containing 2 μg/ml antibody (c,d,g,h); C105, 0.25 μg/ml (f,i); 6-11B-1, $1:10^5$ (j,m); PAT, $1:5\times10^3$ (k,l,n,o); PAT 1, 2 μg/ml (p-s); PAT 2, 0.2 μg/ml (t-w). The apparent molecular masses of the immunoreactive peptides, schematically represented in Fig. 4, are indicated on the right. Note: (1) the upward shifts of the AXO 49 immunoreactive α 19 and β 21 kDa peptides with respect to their staining by C85 and C105 anti-sequence antibodies (lanes b,c and h,i); (2) the downward shifts of Ct α peptides from 19 to 18 kDa (b,e) and of β peptides from 21 to 19 kDa (i,f) following double proteolysis; (3) the identity in migration and reactivity of α Nt 34 and 30 kDa peptides with 6-11B-1 (j,m), PAT (k,l), PAT 1 (p,q), PAT 2 (t,u) after double proteolysis; (4) the reactivity of PAT 1 which is intermediate between those of PAT and AXO 49: the α_s 18 and β_s 19 kDa peptides are much more weakly stained than with the serum (compare lanes p,q with c,d and k,l; and lanes r,s with g,h and n,o); (5) the similarity of PAT 2 reactivity with respect to PAT (compare lanes t,u with k,l; and v,w with n,o).

the locations of the subtilisin cleavage sites in mammalian brain tubulin, probably partly due to different conditions used. On the one hand, from SDS-PAGE (Serrano et al., 1984a) and amino acid analysis (Maccioni et al., 1986), these sites were previously located at positions lying from 30 to 40 residues from the Ct end. On the other hand, native gel electrophoresis (Sackett et al., 1985) and reactivity of site-directed antibodies (de la Vina et al., 1988; Paschal et al., 1989; Lobert et al., 1993) indicated the occurrence of one or several cleavage sites between residue 430 and the end of each subunit. Our results on *Paramecium* tubulin are consistent with the second set of data as well as with the direct determination of the major cleavage sites in pig brain α- and β-tubulin, by sequencing, at positions Asp 438-Ser 439 and Gln 433-Gly 434, respectively (Redeker et al., 1992).

AXO 49 mAb and a fraction of PAT serum are unreactive with bacterially expressed tubulin

Fusion peptides comprising various segments of ciliate (*Stylonychia*) α-tubulin were expressed in *E. coli* and permitted to cover the α-tubulin sequence of ciliates except for the 21 Nt amino acids and the central segment 177-213 (Fig. 4). Their relative migrations after SDS-PAGE are shown in Fig. 5, beside *Paramecium* axonemes (CB, lanes a-f).

After immunoblotting with TU-01 mAb, directed towards an N-terminal sequential epitope of α-tubulin (Grimm et al., 1987), only the Nt fusion peptide, N, is reactive, as expected, similarly as whole α-tubulin from *Paramecium* axonemes (TU-01, lanes a,b,d). With DM1A, all of the Ct fusion peptides embracing the sequence 426-430 are reactive, similarly as α-tubulin (DM1A, lanes a-f).

In contrast to the anti-sequence antibodies, AXO 49 is fully unreactive with all fusion peptides (AXO 49, lanes a,b,d). The lack of reactivity of the fusion peptide C, covering the sequence 214-445, potentially bearing the epitope, as inferred from peptide mapping of axonemal tubulin, was ascertained by probing it at an amount 30-fold greater than that shown here.

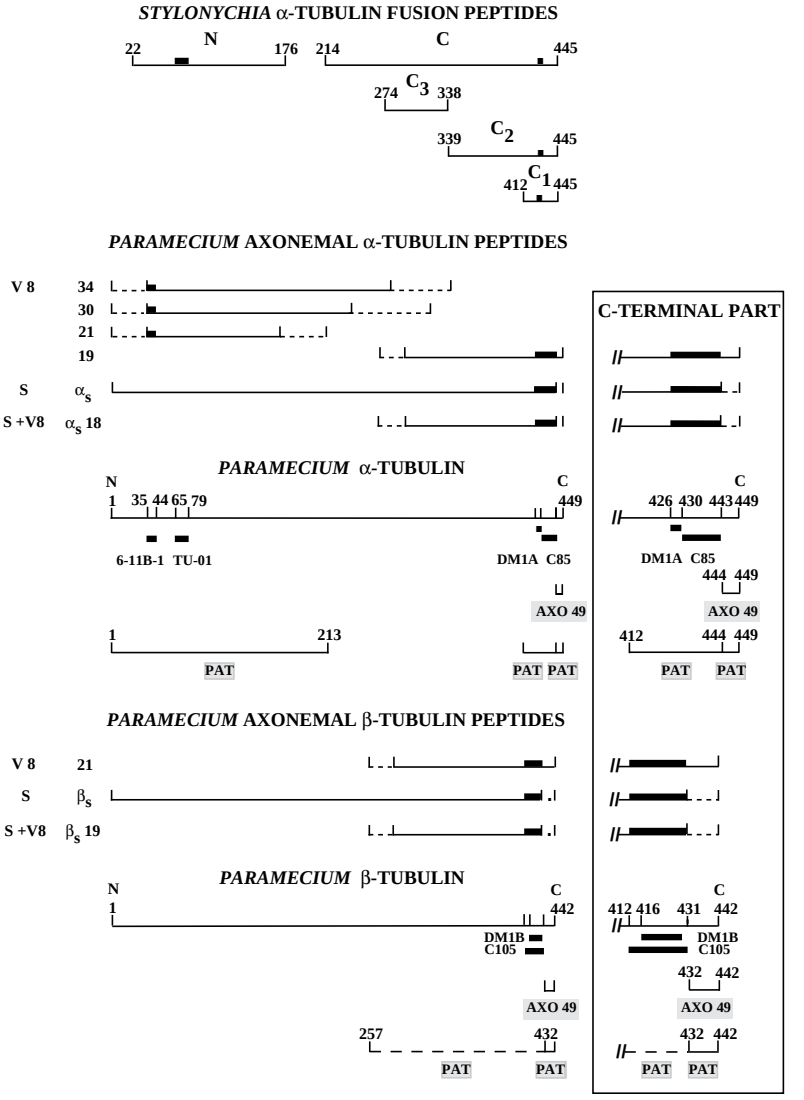

Fig. 4. Schematic localization of the *Paramecium* axonemal α- and β-tubulin antigenic determinants described in this paper. The diagram represents: (1) the structure of fusion peptides generated in *E. coli* from *Stylonychia* α-tubulin gene fragments; (2) *Paramecium* axonemal α- and β-tubulin peptides yielded after proteolysis by V8 protease (V8), subtilisin (S), and subtilisin followed by V8 protease (S+V8). The apparent molecular masses of the peptides, indicated on the left, were determined from their migration after SDS-PAGE. The peptide positions were inferred from their antigenic reactivities with reference antibodies, and dotted lines represent the intervals between their extreme possible positions (see Callen et al., 1994). The epitope positions of the reference antibodies were in most cases determined on vertebrate tubulin from the smallest reactive peptides: 6-11 B-1, α 35-44 (LeDizet and Piperno, 1991); TU-01, α 65-79 (Grimm et al., 1987); DM1A, α 426-430, and DM1B, β 416-430 (Breitling and Little, 1986); C85, α 430-443, and C105, β 412-431 (Arévalo et al., 1990). They are represented on *Stylonychia* α-tubulin fusion peptides, on the whole polypeptidic chains of *Paramecium* tubulin and on their fragments by solid rectangles. The epitope positions of AXO 49 mAb and PAT serum are inferred from their reactivities over *Paramecium* tubulin peptides (see Figs 2, 3) and over fusion peptides (see Fig. 5) and include the uncertainties in the positions of the smallest reactive peptides. The inset figures an enhanced representation of the C-terminal part of the tubulin subunits and peptides showing the epitope positions of the different antibodies. Thanks to the availability of antibodies directed against very Ct sequential epitopes of tubulin and to the use of subtilisin + V8 protease which yielded α_s 18 and β_s 19 kDa peptides devoid of their extreme Ct part comprising the epitopes recognized by AXO 49, the α 19 and β 21 kDa peptides generated by V8 protease and containing the epitopes recognized by AXO 49 are assumed to have retained their Ct end. These peptides are the same as in Callen et al. (1994) except that the presence of their Ct part was not assured at that time and that the latter was formerly represented by dotted lines. Because of the very weak reactivity of the β_s and β_s 19 kDa peptides with PAT, the presence of an antibody directed to an epitope of β-tubulin located upstream of the subtilisin cleavage site cannot be ascertained, hence the representation of the presumptive epitope by a stippled line.

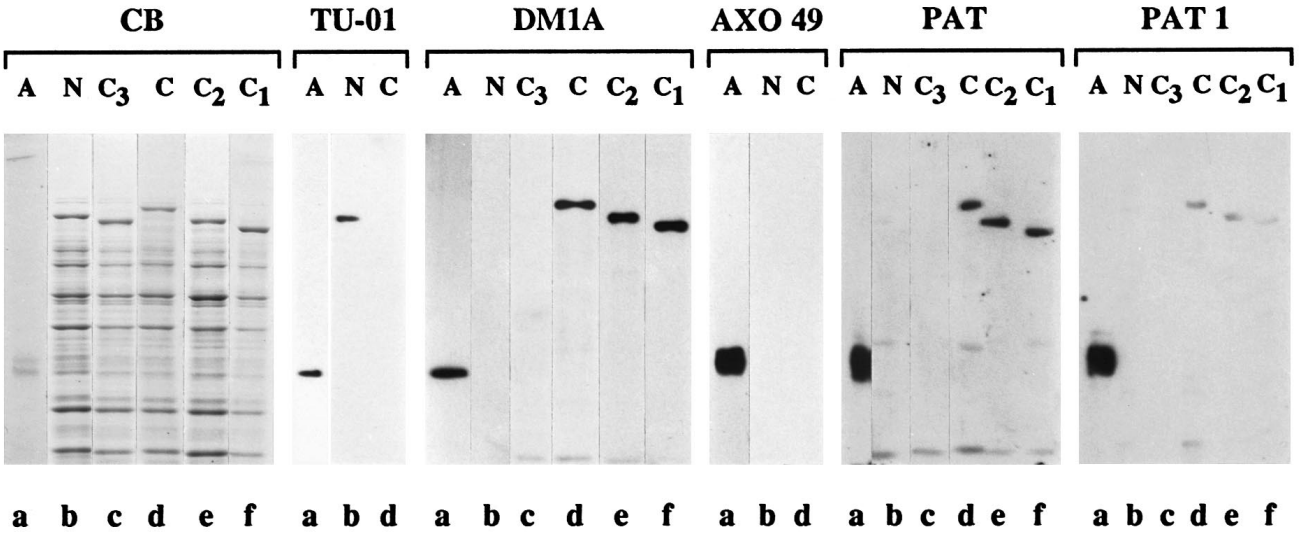

Fig. 5. Immunoblotting analysis of *Stylonychia* α-tubulin fusion peptides (schematized in Fig. 4). Lanes a, *Paramecium* axonemes (A), 0.3 µg. In the other lanes, the fusion protein molar amounts loaded, determined from gel scannings, were equivalent to that of each tubulin subunit. Lanes b, Nt peptides (N); lanes c, internal peptides (C_3); lanes d, large Ct peptides (C); lanes e,f, smaller Ct peptides (C_2, C_1). CB, Coomassie Blue-stained mini-gel. Notice the high apparent molecular masses of fusion peptides due to their coupling to β-galactosidase. Antibody dilutions: TU-01, $1:10^4$; DM1A, $1:5\times10^4$; AXO 49: 1:50; PAT, $1:10^4$; PAT 1, 2 µg/ml. Note the equivalent staining of *Paramecium* axonemal tubulin and of fusion peptides provided by anti-sequence antibodies directed against the α subunit (TU-01, a,b; DM1A, a,d-f). In contrast to the latter antibodies, AXO 49 mAb and PAT serum label both tubulin subunits of *Paramecium* axonemes; the latter appear as a single thick band (AXO 49, PAT, PAT 1, a) at the long exposure times used in order to ascertain the lack of reactivity of AXO 49 with the fusion peptides.

As concerns the whole serum, it is clearly reactive with all of the α Ct fusion peptides comprising the sequence 412-445, but neither reacts with the Nt peptide, N, nor with an internal peptide, C_3, covering the sequence 274-338 (Figs 4 and 5, PAT, lanes a-f). PAT 2 fraction from the serum, which exhibits the same reactivity as the latter on subtilisin-V8 protease peptide maps, is similarly reactive with the α Ct fusion peptides (not shown). In contrast, PAT 1, enriched in AXO 49-like antibody (see Fig. 3), stains very weakly the α Ct fusion peptides (Fig. 5, PAT 1, lanes a-f) in comparison with *Paramecium* axonemes.

Therefore, the lack of reactivity of AXO 49 mAb and of a fraction of PAT serum with ciliate α-tubulin fusion peptides reveals that they very likely are both directed to post-translational epitopes present in *Paramecium* axonemal tubulin (near the C-terminal end of both subunits). In contrast, the reactivity of the whole serum with fusion peptides indicates that it additionally contains (at least) one antibody directed to the α-tubulin sequence 412-445, which is thus further narrowed with respect to the broad localization (267-443) inferred from V8 protease and subtilisin cleavage sites (Fig. 4). In order to account for the weak residual labelling of the Ct β_s peptide, the same antibody could be involved in the recognition of an homologous β-tubulin sequence; alternatively, this may be due to a β sequence-specific antibody. Finally, another antibody directed to an N-terminal region (1-213) of the α subunit has to be considered, but the non reactivity of the serum with the Nt fusion peptide, N, limited to the sequence portion 22-176 (Fig. 4), does not permit us to infer the nature of the epitope involved.

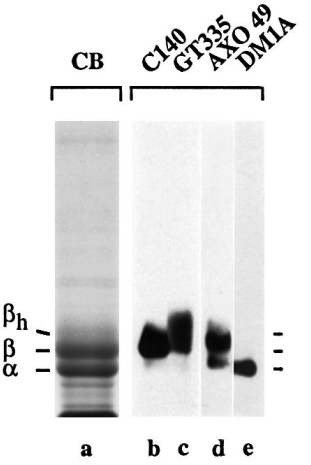

Fig. 6. Compared immunoblotting of *Paramecium* axonemes with GT335 and AXO 49 mAbs. Protein amounts: CB, Coomassie Blue, 15 µg axonemes, corresponding to 7.5 µg tubulin (a); immunoblotting, 1.5 µg axonemes/well (b-e). Antibody dilutions: C140, 0.1 µg/ml (b); GT335, $1:5.10^3$ (c); AXO 49, 1:20 (d); DM1A, $1:5\times10^4$ (e). Lanes b and c, d and e are paired half-tracks which permit us to ascertain the upward shift of GT335 and AXO 49 reactivities with respect to those of C140 and DM1A, respectively. A shift of AXO 49 reactivity with respect to DM1A was similarly observed with purified axonemal tubulin (Fig. 2, lanes a, b).

The target of AXO 49 is different from the polyglutamylation recognized by GT 335 mAb

As polyglutamylation was the most important PTM of tubulin yet found in both subunits, it was crucial to determine whether it corresponded to the epitopes investigated here. Therefore the reactivity of GT335 mAb, directed against tubulin glutamylation (Wolff et al., 1992), was compared to that of AXO 49 on immunoblots of whole or proteolyzed axonemal tubulin.

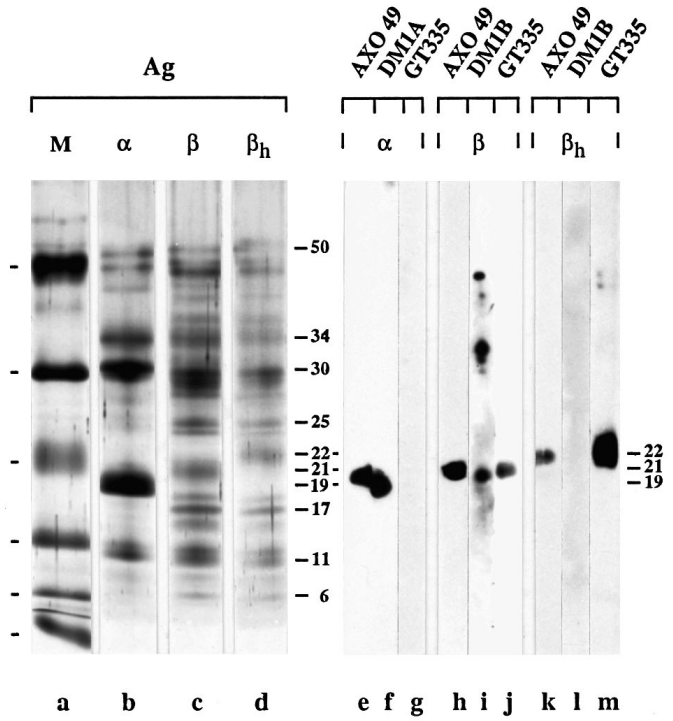

Fig. 7. Silver-stained V8 protease peptide map of *Paramecium* axonemal α-, β- and β_h-tubulins and comparative immunoblotting with AXO 49 and GT335 mAbs. Lane a (M), Rainbow markers as in Figs 1, 3; in the other wells, α-, β- or β_h-tubulin bands from gels loaded with 15 μg axonemes (as in Fig. 6, lane a) were digested with 0.002 μg V8 protease. Ag, silver-stained gel. The apparent molecular masses of the main bands are indicated on the right of lane d. Notice: (1) the typical proteolysis pattern of α-tubulin clustered in few molecular mass zones, of 34-30, 19 and 11 kDa (b), contrasting with the spread pattern of β-tubulin in which peptides of 34, 30, 25, 21, 17, 11 and 6 kDa nevertheless stand out (c); (2) the similarity between the proteolysis patterns of the β and β_h species except for the 21 and 22 kDa peptides, respectively (c,d). Antibody dilutions: AXO 49, 1:10 (e,h,k); DM1A, $1:2\times10^4$ (f); GT335, $1:2.5\times10^3$ (g,j,m); DM1B, $1:10^3$ (i) or 1:500 (l). The apparent molecular masses of the immunoreactive peptides are indicated on the right of lane m. In order to ascertain the differences in mobilities of the peptides reactive with the various mAbs, paired half-tracks originating from a same track cut after transfer were used. Thus: (1) α peptides from paired half-tracks were first incubated with AXO 49 and GT335 (e,g) and the latter one was reincubated with DM1A (f). The staining of the α Ct 19 kDa peptide with AXO 49 is shifted upwards with respect to that yielded by DM1A (e,f), as is also observed using another anti-sequence antibody, C 85 (see Fig. 3b,c). GT335 does not stain the α peptides (g), as expected from its lack of reactivity at the level of the whole α subunit (see Fig. 6c,e). (2) β peptides from paired half-tracks were blotted with DM1B and GT335 (i,j); the staining of the β Ct 21 kDa peptide with GT335 is upward shifted with respect to that yielded by DM1B, similar to AXO 49 staining (h); such a shift has also been observed using AXO 49 and another anti-sequence antibody, C 105 (see Fig. 3h,i). (3) β_h peptide-containing paired half-tracks were first incubated with DM1B and GT335 (l,m) and the former one reincubated with AXO 49 (k). DM1B was fully unreactive, although probed at high concentration. Note that the staining of the β_h Ct 22 kDa peptide with GT335 extends higher than with AXO 49 (k,m), similar to that observed for the whole β_h isoforms (see Fig. 6c,d).

When large amounts of *Paramecium* axonemes are separated after SDS-PAGE, an upward spread of staining is visible above the major α- and β-tubulin species, and a third minor diffuse band, β_h, can be resolved above the level of the β band (Fig. 6CB, lane a).

Immunoblotting of *Paramecium* axonemes with GT335 yields a remarkable staining beginning slightly above the level of β-tubulin located by means of C140 antibody, directed to the β-tubulin sequence 153-165 (Arévalo et al., 1990); this staining is either spreading upward or appearing as a doublet (as observed by Bré et al., 1994) the slower component of which migrates at the level of β_h (lanes a-c). The latter species likely represents (an) isoform(s) of β-tubulin, given that C140 can yield a spread staining extending up to its level, provided that the antigen and antibody concentrations are adequately adjusted. At the level of the α subunit, located with DM1A, no staining is detected with GT335 (lanes c,e). In contrast, with AXO 49, a labelling of both subunits is conspicuous, and again slightly upwards shifted with respect to that yielded by the anti-sequence antibodies (lanes b,d,e). The staining of the α and β subunits is also spread upward and extends to the level of the β and β_h bands, respectively.

V8 protease peptide mapping shows that the proteolysis pattern of the β_h species is very different from that of α-tubulin (Fig. 7, lanes b,d), but resembles that of β-tubulin, except for a β_h 22 kDa peptide which exhibits a higher apparent molecular mass than the corresponding β 21 kDa peptide (lanes c,d). This confirms that the β_h species represents (a) modified isoform(s) of β-tubulin.

Comparative immunoblotting of peptide maps of *Paramecium* axonemal α-, β- and β_h-tubulins with AXO 49 and

Fig. 8. Projections of *Paramecium* cells single labelled with PAT (A,B), DM1A (C), AXO 49 (D,E) and 6-11B-1 (F) anti-tubulin antibodies, or double labelled with PAT (G) and AXO 49 (H) antibodies. Detection was performed using a fluorescein-labelled secondary antibody for single staining, or Texas Red and fluorescein-conjugated secondary antibodies for double staining with PAT serum and AXO 49 mAb, respectively. (A,B) Two respective projections of the same cell at the level of the ventral surface (A) and deeper in the cell (B). Most cilia are strongly decorated with PAT (1:200) along their whole length, except in the anterior left area where they are more weakly decorated (arrow in A). The postoral fiber (Po) emanating from the oral area (O) and the MTs associated with the contractile vacuole system (Cv) are slightly decorated (B). (C) Projection showing the internal network of MTs labelled with DM1A (1:500). Only the tips of the cilia (arrowheads) are decorated under the fixation conditions used. (D,E) Two respective projections of a cell at the level of the ventral surface (D) and deeper (E). Most cilia are decorated with AXO 49 (1:5) more strongly at their proximal than at their distal part (E), except in the anterior left area where they are strongly decorated along their whole length (arrows in D and E). The oral apparatus (O) which includes many cilia, the postoral fiber (Po) and the MTs associated with the contractile vacuole system (Cv) are decorated (E). (F) Projection showing the acetylated microtubular networks labelled with 6-11B-1 (1:100): the postoral fiber (Po), the cytopharyngeal fibers (Cf) and the MTs associated with the contractile vacuole system (Cv). The tips of the cilia are decorated (arrowheads). (G,H) Projections at the same level of a dividing cell double-labelled with PAT serum (G) and AXO 49 mAb (H). In (G), PAT decorates the cytospindle (arrows) as well as the parental (P) and the newly assembled (N) vacuole systems; in (H), AXO 49 only decorates the parental (P) vacuole systems. Bars, 25 μm.

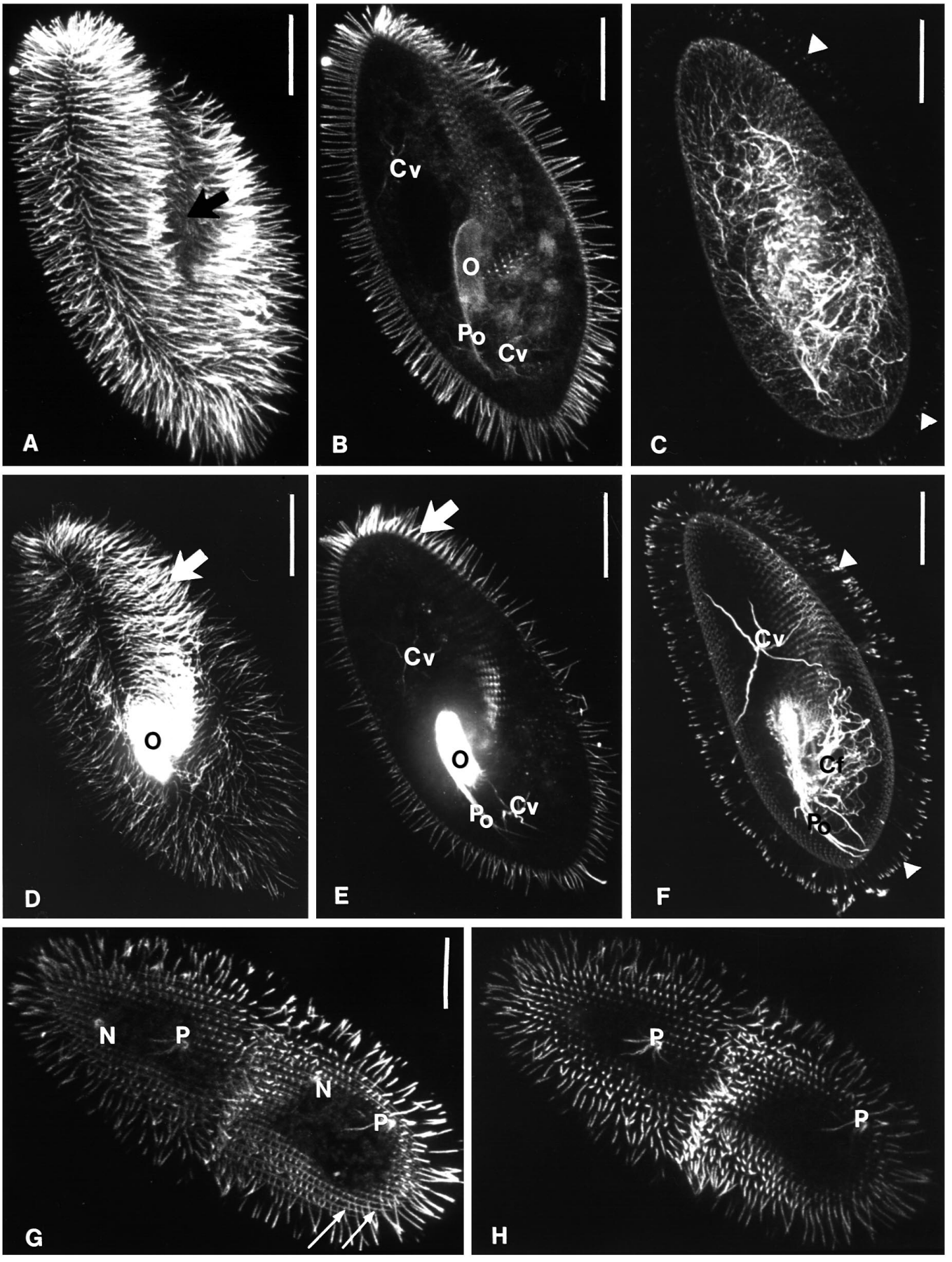
A
B
Cv
O
Po
Cv
C
D
O
E
Cv
O
Po
Cv
F
Cv
Cf
Po
G
N
P
N
P
H
P
P

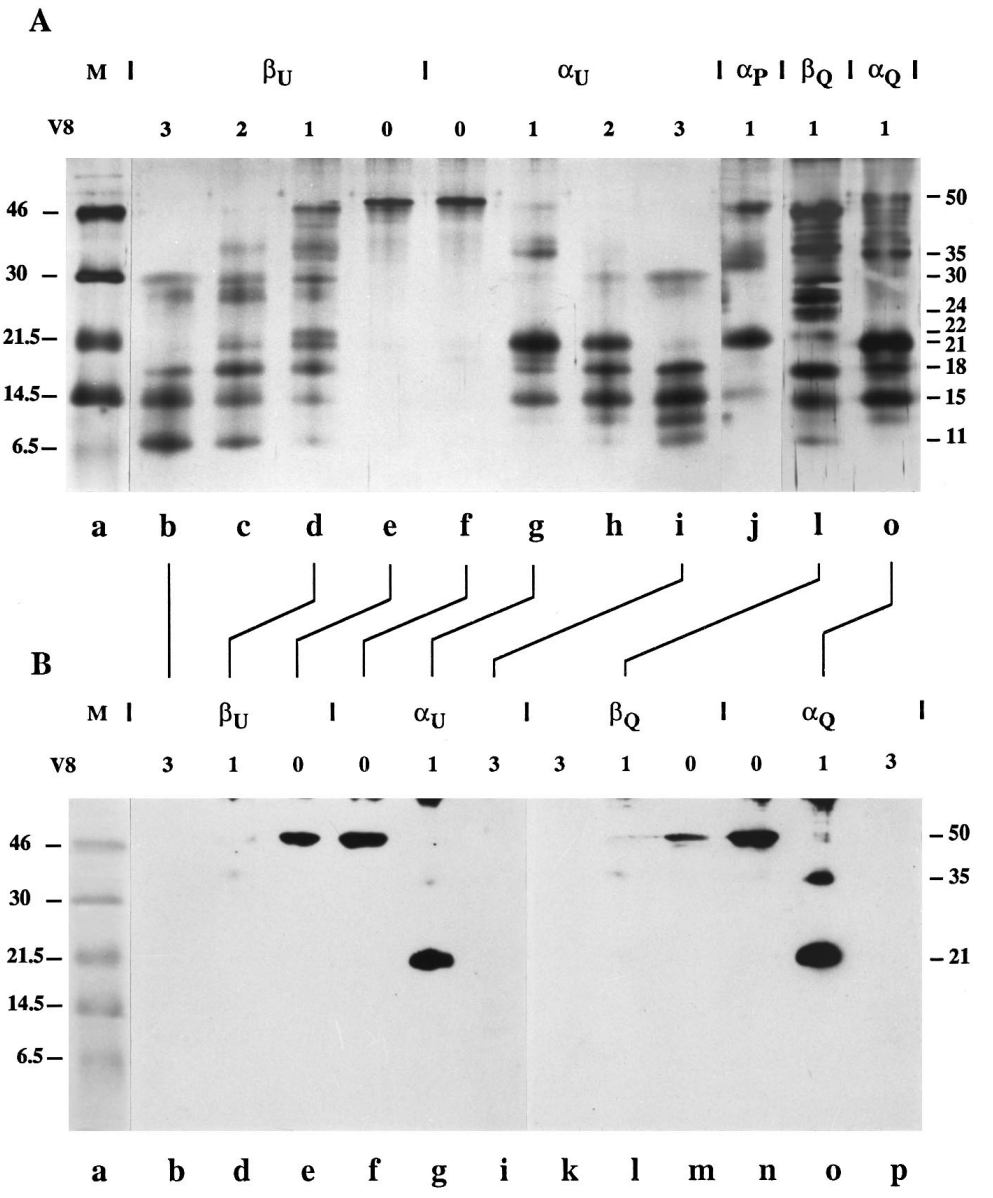

Fig. 9. Comparative silver-stained V8 protease peptide maps of axonemal α- and β-tubulins from sea urchin spermatozoa and quail oviduct cilia (A) and immunoblotting with AXO 49 mAb (B). Lanes a (M), Rainbow markers with their molecular masses (in kDa) shown on the left. In the other lanes, tubulin bands from gels of axonemes of sea urchin (β_U, α_U), *Paramecium* (α_P), and quail (β_Q, α_Q) were, respectively, digested with various amounts of V8 protease, denoted as in Fig. 1. In (A) and (B), lanes containing identical proteins and protease amounts are joined by means of lines and identified with the same letters. The apparent molecular masses of the main peptides and those of the peptides immunoreactive with purified AXO 49 mAb (50 μg/ml) are, respectively, indicated on the right of (A) and (B). In (A), notice: (1) the numerous β-tubulin peptides from sea urchin (b-d) and quail (l), particularly visible at low protease concentration and high protein loading (l); their molecular masses cover the 50-35, 30-24, 22, 18, 15, and 11 k Da ranges, as also observed with the *Paramecium* β peptides (Fig. 7c); (2) the small number of major α-tubulin peptides from sea urchin, *Paramecium* and quail; they display molecular masses of 35, 21, 18, 15 and 11 kDa (g-j,o); (3) the lack of occurrence of metazoan α-tubulin peptides in the 25 kDa range (g-i,o; Adoutte et al., 1991), in contrast to *Paramecium* (Fig. 7b; Callen et al., 1994). It should be noted that differences are found between apparent molecular masses of peptides determined from peptide maps of *Paramecium* and of metazoan tubulins. These result from the different migration rates of the peptides with respect to those of the molecular mass markers under the different gel conditions, respectively, used in both cases (see Materials and Methods). Therefore the former α 34, 30, 19 and 11 kDa peptides from *Paramecium* tubulin (Figs 1, 3, 7; Callen et al., 1994) are the same ones as the 35, 32, 21 and 15 k-Da ones from *Paramecium* and metazoan tubulins observed here (Figs 9, 10) and in Adoutte et al. (1991). Similarly, the former β 21 kDa *Paramecium* peptide is here referred to as 22 kDa peptide. In (B), notice the strong AXO 49 reactivity with α 21 kDa peptides from axonemal tubulins of sea urchin and quail which are the major ones in the corresponding peptide maps (A and B, lanes g,o) as in the case of *Paramecium* (A, lane j). The lack or weakness of staining of β 22 kDa peptides (B, lanes d,l) from the metazoan tubulins contrasts with the strong staining of the corresponding α peptides, as well as of the β 21 kDa peptide from *Paramecium* (Fig. 1d). It can be explained by: (1) the important difference between the amounts of the metazoan β and α peptides (in A, compare lanes d and g,l and o), still more pronounced than in the case of *Paramecium* (Fig. 7b,c), and (2) the lower reactivity of the uncleaved sea urchin and quail β subunits with respect to the α ones (in B, compare lanes e with f,m with n), and to *Paramecium* β-tubulin (compare lanes e and m with lane e of Fig. 1).

GT335 shows that: (i) in contrast to GT335, which is unreactive, AXO 49 strongly labels the α Ct 19 kDa peptide; moreover, this staining is shifted upward with respect to that provided by DM1A (lanes e,f,g). (ii) The β Ct 21 kDa peptide is reactive with GT335 as well as with AXO 49, and the staining yielded by both mAbs is slightly upward shifted with respect to that provided by DM1B (lanes h-j). (iii) Remarkably, the β_h 22 kDa peptide, which is neither stained by DM1A (not shown) nor by DM1B, is nevertheless fairly reactive with AXO 49 and especially with GT335 (lanes k-m), indicating that it is C-terminal. Taking into account the relative amounts of the α, β and β_h Ct peptides (lanes b-d), it can be inferred that AXO 49 reactivity is actually stronger at the level of the β and β_h species than that of the α one, whereas GT335 reactivity is the highest with the slower migrating isoform(s) of tubulin, β_h.

AXO 49 and PAT label a subpopulation of stable microtubular arrays in *Paramecium*

The labelling of *Paramecium* cells by AXO 49 and PAT displays very characteristic features which are completely different from those provided by other antibodies, either directed against sequential or post-translational epitopes of tubulin.

These antibodies are the only ones which strongly label the ciliary axonemes along their length, except their tip (Fig. 8A,B,D,E). In contrast, the anti-sequence antibodies, such as DM1A, strongly label only the tip of the cilia (along ~2 μm length), similar to 6-11B-1 (Fig. 8C,F; Adoutte et al., 1991) and other anti-sequence and anti-acetylated α-tubulin mAbs (Callen et al., 1994) while GT335 labels both the axoneme proximal part and the tip (Bré et al., 1994). Moreover, all cilia are not similarly labelled with AXO 49 and PAT. Those from the anterior left area of the cell are more brightly stained with AXO 49, and less intensely with PAT, whereas the reverse is true for the cilia located in the other cortical areas (Fig. 8A,D). Strikingly, the largest part of the anterior left cell area, where no basal body duplication occurs during division, has specific invariant morphogenetic properties (Iftode et al., 1989).

Contrary to DM1A which decorates all microtubular networks in *Paramecium*, and in particular the intracytoplasmic labile one, AXO 49 and PAT do not label cytoplasmic MTs (Fig. 8B,C,E), in agreement with blotting data (M. H. Bré, personal communication). Similarly, 6-11B-1 does not label the cytoplasmic MTs (Fig. 8F; Adoutte et al., 1991) and very weakly labels cytoplasmic tubulin on immunoblots (Callen et al., 1994). In contrast, a fraction of cytoplasmic MTs is recognized by GT335 (Bré et al., 1994).

The labelling of *Paramecium* cells with AXO 49 and PAT is limited to very stable MTs, associated with the cortex and probably the membranes, and usually found as bundles. In addition to axonemes, it comprises particularly the contractile vacuole system and the postoral fiber; this population of stable MTs is more restricted than that recognized by 6-11B-1 (Fig. 8B,E,F; Adoutte et al., 1991) or by GT335 (Bré et al., 1994).

In the course of cell division, the reactivity of the new microtubular structures with PAT is detected only after a certain lag time following their assembly revealed by their reactivity with DM1A or DM1B (Adoutte et al., 1991). Two differences between AXO 49 and PAT are clearly visualized by double labelling experiments (Fig. 8G,H). On the one hand, the cytospindle, consisting of a transient set of cortical MTs assembling beneath the cortex during division, is unreactive with AXO 49 while labelled with PAT. On the other hand, the new microtubular structures, such as the contractile vacuole system, become reactive with AXO 49 still later than with PAT.

The epitopes detected in *Paramecium* with AXO 49 and PAT are present in axonemal tubulin of metazoa

As PAT serum reacts with axonemal tubulins of metazoa (Adoutte et al., 1985), we tested AXO 49 mAb in comparison with the serum on peptide maps of axonemal tubulins from an invertebrate and from a vertebrate, i.e. those from sea urchin spermatozoan flagella and from quail oviduct cilia.

The V8 protease cleavage patterns of axonemal β-tubulins from sea urchin (Fig. 9A, lanes a-e), quail (lane l; Adoutte et al., 1991) and *Paramecium* (Fig. 7, lane c; Callen et al., 1994) display a distribution of numerous peptides of various mobilities, whereas the corresponding α-tubulins yield, after proteolysis, a few groups of major peptides (Fig. 9A, lanes f-j,o; Adoutte et al., 1991; Callen et al., 1994). Such differences had been previously observed between cleavage patterns of β- and α-tubulins from protists to metazoa (Little et al., 1981; Adoutte et al., 1985).

Both subunits of sea urchin flagellar tubulin are reactive with AXO 49, whereas only α-tubulin of quail cilia is clearly reactive (Fig. 9B, lanes e,f,m,n).

After proteolysis, AXO 49 strongly reacts with α-tubulin 21 kDa peptides from both species which are the major ones present in the corresponding peptide maps (Fig. 9A,B, lanes g,o), as in the case of *Paramecium* (Fig. 9A, lane j and Fig. 1, lane g). AXO 49 also weakly reacts with minor α-tubulin 35 kDa peptides from both metazoan species, but not from *Paramecium* (Fig. 9B, lanes g,o and Fig. 10, lanes d-f). Both 21 and 35 kDa peptides, labelled by DM1A (Fig. 10, lanes d,j), are C-terminal. PAT serum, like AXO 49 mAb, labels strongly the major Ct 21 kDa peptides from metazoan and *Paramecium* axonemal tubulins, and weakly the minor Ct 35 kDa peptides from metazoan tubulin (Fig. 10, lanes d-i). In addition, PAT labels supplementary

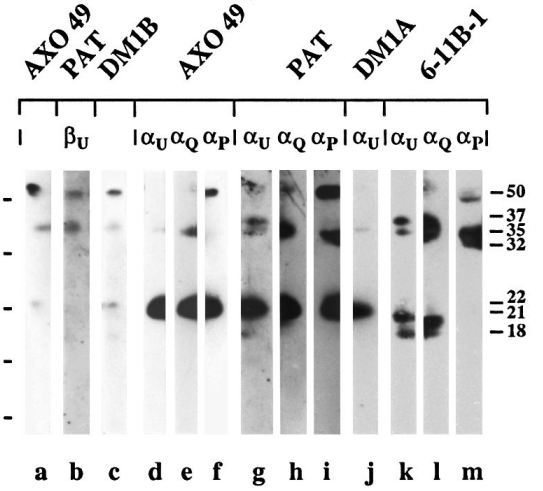

Fig. 10. Comparative immunoblotting of peptide maps of axonemal tubulins from sea urchin spermatozoa, quail oviduct and *Paramecium* cilia with AXO 49 mAb and PAT serum. The positions of the rainbow markers (as in Fig. 9) are indicated on the left, and the apparent molecular masses of the immunoreactive peptides are shown on the right. Tubulin bands from axonemes of sea urchin (β_U, α_U), quail oviduct (α_Q) and *Paramecium* (α_P) were digested with 0.002 μg V8 protease. Antibody dilutions: AXO 49, 1:10 (a,d-f); PAT, $1:2\times10^3$ (b,g-i); DM1B, $1:5\times10^3$ (c); DM1A, $1:5\times10^4$ (j); 6-11B-1, $1:8\times10^3$ (k-m). For comparison of AXO 49 mAb and PAT serum reactivities, paired half-tracks were used for β_U (a,b), α_U (d,g), α_Q (e,h), α_P (f,i). For comparison of PAT serum and 6-11B-1 mAb, double labelling was performed with 6-11B-1 following PAT reactivity detection. Note that: (1) the staining of metazoan tubulin α peptides by PAT in the 35-37 kDa range (g,h) results from the overlapping of the labelling of Ct 35 kDa peptides (j), also reactive with AXO 49 (d,e) and of Nt 35 and 37 kDa peptides, reactive with 6-11B-1 (k,l). In contrast, in the case of *Paramecium*, only Nt peptides are present in this range, which are stained by PAT and 6-11B-1 (i,m). (2) Smaller Nt peptides, of 18 and 19 kDa, reactive with 6-11B-1, are present in the metazoan tubulins only (k-m), whereas in *Paramecium*, a 21 kDa Nt peptide is mainly occurring at high protease concentration (Callen et al., 1994); the 18 and 21 kDa peptides are weakly stained by PAT (g,h and Fig. 1, lane q).

peptides. These are 6-11 B-1 reactive metazoan tubulin 37, 35 and 18 kDa Nt peptides, and *Paramecium* tubulin 32-35 kDa peptides (lanes g-i, k-m) as is also a 21 kDa one, observed at high protease concentration (Fig. 1, lane q).

On peptide maps of axonemal β-tubulins from sea urchin and quail, 36 and 22 kDa C-terminal peptides are very weakly stained by AXO 49, PAT and DM1B (Fig. 9B, lanes d,l and Fig. 10, lanes a-c). The very weak staining of the metazoan β-tubulin 22 kDa peptides contrasts with the strong labelling of the corresponding α 21 kDa peptides, as well as of the *Paramecium* β-tubulin 21 kDa peptide (Fig. 1, lanes d,l). This cannot be accounted for solely on the basis of differences in amounts of the corresponding peptides (see below).

In conclusion: (1) in spite of an overall resemblance in the metazoan and protozoan axonemal α-tubulins, mainly yielding Nt 35 kDa and Ct 21 kDa complementary peptides, additional Ct 35 kDa and Nt 18 kDa complementary fragments were detected in the metazoan tubulins only (Fig. 9A, lanes g-j,o, and Fig. 10, lanes j-m). These observations are in agreement with those of Little et al. (1984a) showing differences between the proteolysis patterns of axonemal α-tubulins from metazoa and protozoa, contrasting with the resemblance of the β-tubulin patterns. (2) The similar reactivity of AXO 49 mAb and PAT serum with axonemal α-tubulin Ct 21 kDa peptides from metazoa and *Paramecium* permits us to: (i) extend to metazoa the presence of the post-translational epitopes detected in *Paramecium*, and (ii) narrow their localization near the α-tubulin C-terminal end in these metazoa. As for the β subunit, the very weak reactivity of the metazoan Ct peptides with AXO 49 and PAT contrasts with the strong reactivity of the *Paramecium* homologue. Therefore, in these metazoan species, either the β-tubulin post-translational epitopes are less abundant than in *Paramecium*, or they differ in such a way that their affinity for both antibodies is weaker. (3) The secondary reactivity of the PAT serum with metazoan α-tubulin Nt 18 kDa peptides whose sequence position, 1-203 (determined as by Callen et al., 1994), overlaps with the N-terminal epitope location (1-213) found in *Paramecium* α-tubulin, suggests a conservation of the latter epitope in metazoan α-tubulins.

DISCUSSION

AXO 49 mAb and PAT serum reveal a post-translational modification of tubulin in axonemes and other stable microtubular arrays

In ciliated and flagellated cells of both protists and metazoa, a range of data involving cleavage pattern similarities (Little et al., 1982; Russell et al., 1984), reflagellation studies (McKeithan et al., 1983; Russell and Gull, 1984), tubulin gene homogeneity and tubulin isotype multifunctionality (Little et al., 1984b; Raff, 1984; Joshi and Cleveland, 1990; Silflow, 1991; Gaertig et al., 1993; Luduena, 1993; Renthal et al., 1993) have provided evidences that axonemal tubulin is drawn from the same pool as the cytoplasmic one and is then post-translationally modified.

In this context, the reactivity of axonemal MTs of *Paramecium* and metazoa with AXO 49 mAb and PAT serum, combined with the lack of reactivity of their respective cytoplasmic counterparts with AXO 49 (this report) and with PAT (Adoutte et al., 1985, 1991), strongly suggest that both antibodies recognize a post-translational modification of axonemal MTs occurring on the same tubulin species as those involved in the cytoplasmic pool. The alternative hypothesis, which could account for the specificity of our antibodies, namely the recognition of axonemal-specific isotypes, does not hold by reason of the lack of homologous sequences in the C-terminal part of α- and β-tubulins from *Paramecium* (Dupuis, 1992a,b) and from metazoan testis-specific isotypes (Little and Seehaus, 1988) which could distinguish them from other isotypes (Fig. 11).

The non reactivity of AXO 49 mAb and of a fraction of PAT serum over ciliate α-tubulin expressed in *E. coli* as fusion protein, conjugated with their reactivity with *Paramecium* axonemal α- and β-tubulin, provide decisive evidence permitting us to affirm that both antibodies are directed against a post-translational modification present in both subunits of axonemal tubulin, not occurring in bacteria. Effectively, we have previously shown that, given the great conservation of ciliate tubulin, antibodies directed against tubulin sequential epitopes (including conformational determinants) were indeed reactive with bacterially expressed ciliate tubulin whereas, conversely, antibodies directed against PTMs of tubulin proved to be totally unreactive (Callen et al., 1994), even with large amounts of fusion protein like those probed with AXO 49.

The apparent molecular mass heterogeneity of *Paramecium* axonemal α- and β-tubulin revealed by SDS-PAGE and immunoblotting and its decrease after removal of the Ct end of both subunits concomitant with loss of AXO 49 reactivity (Fig. 2) suggest that different α- and β-tubulin isoforms are generated by successive PTMs located in their C-terminal end which would each cause slight upward shifts in electrophoretic mobility. This assertion is supported by the following observations: (i) an increase in the apparent molecular masses of numerous isoforms of axonemal tubulins as a function of the

```
α Paramecium tetraurelia 1 EGMEEGEFSE AREDLAALEK DYEEVGIETA E**GEGEE*G EG
α Paramecium tetraurelia 2 ---------- ---------- ---------- -**-----*- -A
α Gallus gallus testis 2   --------A- ---------- --d--ATdLF -**D-N-A*- dS
α Gallus gallus brain 1    ---------- ----m----- ------vdsV -**-----E- -EY
β Paramecium tetraurelia 1 ---d-M--t- -ESNmND-VS e-QQYQDA-- -EE--F--E- -Q
β Gallus gallus testis 3   ---d-M--t- -ESNmND-VS e-QQYQDA-- -EE--F--E- -EEAE
β Gallus gallus brain 1    ---d-M--t- -ESNmND-VS e-QQYQDA-- dEQ--F--E- -EDEA
```

Fig. 11. Amino acid sequence comparison of the C-terminal part of *Paramecium* and metazoan (chicken) α- and β-tubulins. Sequences of α1, α2 and β1 isotypes of *Paramecium* tubulin are from Dupuis (1992a,b). Only the regions α 411-449 and β 401-442 are shown here. Sequences of α2 (testis-specific), α1 (mainly brain), β3 (mainly testis), β1 (mainly brain) isotypes of chicken tubulin are from Little and Seehaus (1988). Gaps were introduced in α-tubulin in order to get the best alignment. The lower case letters indicate conservative substitutions. Each subunit contains a conserved region followed by a variable isotype-defining one comprising ~ the 15 last residues. Note: (1) the lack of homologous stretches of at least 5 residues that might constitute sequential epitopes for antibodies cross-reacting with both subunits; (2) the lack of distinct features in tubulin sequences of protist and metazoan testis-specific isotypes which could account for the specific recognition of axonemal tubulin by AXO 49 and PAT antibodies.

glutamylation degree (Bré et al., 1994; Fouquet et al., 1994); (ii) a decrease in brain tubulin isoform amount after subtilisin cleavage (Redeker et al., 1992). Thus the upward shifts of AXO 49 and GT335 reactivities and the lack of shift of PAT reactivity with respect to the staining yielded by anti-sequence antibodies indicate that AXO 49 and GT335 detect only modified isoforms, whereas PAT also reacts with unmodified axonemal tubulin, certainly through its anti-α-tubulin sequence antibodies.

Although acetylation slows down tubulin migration (Callen et al., 1994), this upward shifting of immunoreactive isoforms with respect to the bulk of tubulin cannot be caused by acetylation since: (i) it is also observed at the level of Ct α 19 kDa and β 21 kDa peptides whereas acetylation is located in the Nt domain of α-tubulin (Figs 3, 7); (ii) axonemal tubulin is mostly acetylated so that its labelling with 6-11B-1 and DM1A is observed at the same level (Callen et al., 1994). The apparent molecular mass heterogeneity cannot be accounted for by acetylation either, since there is probably a single acetylation site in *Paramecium* α-tubulin Nt domain, as inferred from brain tubulin (Eddé et al., 1991; Callen et al., 1994).

Remarkably, the high apparent molecular mass isoforms are conspicuously stained by antibodies directed against Nt sequential and post-translational epitopes of α- (Callen et al., 1994) and β-tubulin (such as C140), but are less well or even not labelled by DM1A and DM1B (Fig. 7, lane l); this may reflect either a differential affinity of the antibodies for these minor isoforms or a reduction of accessibility of antibodies towards sequential Ct epitopes by PTMs located in their vicinity (see also Bré et al., 1994).

Therefore, in *Paramecium* axonemal tubulin, in addition to polyglutamylation detected next to and above the level of the β subunit, another C-terminal polymodification, recognized by AXO 49 and PAT, is responsible for the considerable apparent molecular mass heterogeneity and presumably for the reduction of accessibility of Ct sequential epitopes of the α (and β) subunit(s).

The similarly restricted reactivities of AXO 49 mAb and PAT serum with *Paramecium* microtubular networks and their late occurrence during cell division confirm that these antibodies are directed against the same post-translational modification taking place after MT assembly.

The presence of anti-sequence antibodies in the serum can neither account for the opposite relative reactivities of cilia from different parts of the cell with AXO 49 and PAT, nor for the lag time remaining between MT assembly and appearance of PAT reactivity. These observations as well as the delayed reactivity of AXO 49 with respect to PAT, and the non reactivity of transient structures with AXO 49 would be rationalized if AXO 49 recognized a later stage of a multi-step PTM than PAT.

AXO 49 and PAT detect a new post-translational modification of tubulin

Both AXO 49 and PAT decorate, in *Paramecium*, a narrower subpopulation of stable MTs than other antibodies directed to PTMs, namely acetylation and polyglutamylation. Both antibodies yield a unique labelling pattern of *Paramecium* ciliary axonemes, consisting of a strong decoration of the axoneme body except the tip, roughly complementary to those yielded by other anti-tubulin antibodies. This suggests that they are targeted against a bulky modification leading to a decreased accessibility of other antibodies to their epitopes along the axoneme. Although all tubulin PTMs occur preferentially on the MTs (Greer and Rosenbaum, 1989; Audebert et al., 1993; Paturle-Lafanechère et al., 1994), the modification revealed by AXO 49 and PAT is the only one which appears to be delayed with respect to MT assembly (Fleury et al., 1995). These unique immunocytochemical features point to a new type of tubulin modification, distinct from previously known ones.

(1) The *detyrosination-tyrosination* of tubulin, associated with the presence of a Gly-Glu-Glu-(Tyr) sequence, occurs at the C-terminal end of the α subunit in metazoa (Gu et al., 1988; Little and Seehaus, 1988; Rüdiger et al., 1994), and has only been detected in few cases in protists (Stieger et al., 1984; Birkett et al., 1985). In ciliates, it has not yet been found, in agreement with the available sequence data (Fig. 12). Moreover, in *Paramecium*, the anti-tyrosinated tubulin antibody YL 1/2 (Kilmartin et al., 1982; Wehland et al., 1984) is unreactive. In conclusion, the tubulin subunit specificity and the distribution of the detyrosination-tyrosination of tubulin (Barra et al., 1974; Gundersen and Bulinski, 1986), are completely different from those of the modification investigated here.

(2) The same comments can be made for the PTM involving the *removal of a glutamyl-tyrosine dipeptide* at the C-terminal end of the α-tubulin subunit (Paturle-Lafanechère et al., 1994).

(3) The subunit and/or species distribution yet found for *phosphorylation* (see Introduction; and Hirano-Ohnishi and Watanabe, 1989; Matten et al., 1990) do not correspond to those of the modification we are looking for.

(4) We have particularly paid attention to *acetylation* of tubulin, on account of several analogies of this PTM with that revealed in *Paramecium*, namely its detection in cilia, flagella and other stable MTs of metazoa and protists (L'Hernault and Rosenbaum, 1983; LeDizet and Piperno, 1991), including *Paramecium* (Cohen and Beisson, 1988; Torres and Delgado, 1989).

The immunocytochemical and peptide mapping data we obtained here and previously (Adoutte et al., 1991; Callen et

Paramecium tetraurelia 1	AEGEGEE*GEG
Paramecium tetraurelia 2	-------*--A
Tetrahymena pyriformis	-------E-Y
Tetrahymena thermophila	-------E-Y
Stylonychia lemnae 1	V------E-ME
Stylonychia lemnae 2	-------E-ME
Oxytricha granulifera	-------E-ME
Euplotes octocarinatus	-------E-ME
Euplotes vannus	-------EDMA
Blepharisma japonicum	--A----E-Y-EEL
Gallus gallus 1	V------E--EY

Fig. 12. Amino acid sequence comparison of the C-terminal ends of ciliate α-tubulins. Sequence references: *Paramecium tetraurelia* (Dupuis, 1992a); *Tetrahymena pyriformis* (Barahona et al., 1988); *Tetrahymena thermophila* (McGrath et al., 1994); *Stylonychia lemnae* (Heltenbein and Müller, 1988); *Oxytricha granulifera* and *Euplotes vannus* (Gaunitz, 1990); *Euplotes octocarinatus* (Liang et al., 1994); *Blepharisma japonicum* (Liang and Heckmann, 1993); chicken brain (Little and Seehaus, 1988). A gap was introduced in the *Paramecium* sequences in order to improve the alignment. Chicken brain α1-tubulin, which contains the C-terminal sequence GEEY specifically recognized by the detyrosination-tyrosination enzymes, was included as reference.

al., 1994) have shown that the modification revealed by PAT and AXO 49 was different from the acetylation, and that the post-translational epitopes recognized by both antibodies are located near the C-terminal end of both subunits from *Paramecium* and metazoan axonemal tubulins, contrary to the acetylation site which is located in the N-terminal part of the α subunit only.

(5) We have further focussed our attention on *polyglutamylation* which shares some common features with the modification investigated here. It has been detected near the C-terminal end of both tubulin subunits (see Introduction), and in *Paramecium*, the reactivity of GT335 mAb was abolished after subtilisin cleavage (Bré et al., 1994), like that of AXO 49.

However, we have shown that various isoforms of *Paramecium* axonemal tubulin are differentially reactive with GT335 and AXO 49 mAbs. Furthermore, although widely spread among axonemal tubulins (Fouquet et al., 1994), glutamylation also occurs on labile cytoplasmic MTs in *Paramecium* (Bré et al., 1994) and metazoa (Wolff et al., 1992), and is a major PTM of mammalian brain tubulin (Eddé et al., 1991), contrary to the modification recognized by AXO 49 (Callen et al., 1994).

(6) A remaining candidate for the PTM analysed here is the very recently discovered *polyglycylation* (Redeker et al., 1994). The latter has been localized at residues Glu 445 and Glu 437 of *Paramecium* axonemal α- and β-tubulin, respectively, which fits with the location determined here for the epitopes recognized by AXO 49, namely in the sequence segments α(444-449) and β(432-442). The final characterization confirms that the target of AXO 49 indeed corresponds to the polyglycylation (M. H. Bré et al., unpublished). Thus, the potential high degree of polymodification, consisting of the addition of up to 34 glycyl units, and the great diversity of polyglycyl chain lengths displayed (Redeker et al., 1994) can well account for the reduced accessibilities of various antibodies to their epitopes in *Paramecium* axonemal tubulin and axonemes, respectively observed by immunoblotting and immunocytochemistry, and for the considerable apparent molecular mass heterogeneity of axonemal tubulin exhibited on gels and immunoblots. Moreover, the multi-step nature of polyglycylation could account for the sequential appearance of PAT and AXO 49 immunoreactivity in the course of assembly of microtubular structures in *Paramecium*, and also for the non reactivity of some transient structures (such as the cytospindle) with AXO 49; PAT and AXO 49 could recognize differently glycylated forms of tubulin. In addition, the opposite relative reactivities of the cilia with the two antibodies would imply a specific distribution of glycylated forms of tubulin through the cell. It is striking that this differential PTM distribution correlates with specific morphogenetic stability properties of the corresponding cell territories.

Moreover, the extension of AXO 49 reactivity to axonemal tubulins of metazoa, such as sea urchin and quail, indicates that this new PTM revealed by our antibodies is widely spread through evolution.

Our data, by increasing the number of PTMs occurring in the C-terminal end of both tubulin subunits, known to play a regulatory role in MT assembly and dynamics, and also in interactions with MAPs and motor proteins, raises the question of the role of this new modification. The uniqueness of the polyglycylation resides in its occurrence in microtubular assemblies including the most stables ones known, namely the axonemes of cilia and flagella, therefore suggesting, in contrast to others, a possible role of this modification in MT stability. This could be achieved at three levels (Gelfand and Bershadsky, 1991), either by acting directly on polymer stability, or/and indirectly through interactions with associated proteins or with the membrane.

This work was supported by the CNRS and the Université Paris-Sud. We are very grateful to A. Adoutte for his constant encouragements and for his important contribution to this work. We thank particularly J. C. Clérot and R. Jeanmaire-Wolf for the production of AXO 49 mAb without which this work could not have been carried out; A. Baroin-Tourancheau and P. Delgado for the construction of fusion proteins; A. M. Callen for performing experiments with fusion proteins; M. H. Bré for helpful discussions and critical reading of the manuscript; G. Coffe for fruitful discussions and F. Iftode for constant help in *Paramecium* culture. We also would like to thank the colleagues who provided us with protein samples and antibodies. We are grateful to H. Philippe for sharing aligned sequences; M. Laurent for help in confocal microscopy (Service d'Imagerie Cellulaire, Orsay); G. Géraud for his assistance in the use of a two-laser equipped confocal microscope (Service d'Imagerie, Institut Jacques Monod, Paris); G. Johannin for his help in picture scanning (Service d'Imagerie Cellulaire, Orsay); C. Couanon for help in picture and manuscript editing; and N. Narradon for extensive photographic work.

REFERENCES

Adoutte, A., Claisse, M., Maunoury, R. and Beisson, J. (1985). Tubulin evolution: ciliate-specific epitopes are conserved in the ciliary tubulin of metazoa. *J. Mol. Evol.* **22**, 220-229.

Adoutte, A., Delgado, P., Fleury, A., Levilliers, N., Lainé, M. C., Marty, M. C., Boisvieux-Ulrich, E. and Sandoz, D. (1991). Microtubule diversity in ciliated cells: evidence for its generation by post-translational modification in the axonemes of *Paramecium* and quail oviduct cells. *Biol. Cell* **71**, 227-245.

Alexander, J. E., Hunt, D. F., Lee, M. K., Shabanowitz, J., Michel, H., Berlin, S. C., Macdonald, T. L., Sundberg, R. J., Rebhun, L. I. and Frankfurter, A. (1991). Characterization of posttranslational modifications in neuron-specific class III β-tubulin by mass spectrometry. *Proc. Nat. Acad. Sci. USA* **88**, 4685-4689.

Arévalo, M. A., Nieto, J. M., Andreu, D. and Andreu, J. M. (1990). Tubulin assembly probed with antibodies to synthetic peptides. *J. Mol. Biol.* **214**, 105-120.

Audebert, S., Desbruyères, E., Gruszczynski, C., Koulakoff, A., Gros, F., Denoulet, P. and Eddé, B. (1993). Reversible polyglutamylation of α- and β-tubulin and microtubule dynamics in mouse brain neurons. *Mol. Biol. Cell* **4**, 615-626.

Barahona, I., Soares, H., Cyrne, L., Penque, D., Denoulet, P. and Rodrigues-Pousada, C. (1988). Sequence of one α- and two β-tubulin genes of *Tetrahymena pyriformis*. Structural and functional relationships with other eukaryotic tubulin genes. *J. Mol. Biol.* **202**, 365-382.

Barra, H. S., Arce, C. A., Rodriguez, J. A. and Caputto, R. (1974). Some common properties of the protein that incorporates tyrosine as a single unit and the microtubule proteins. *Biochem. Biophys. Res. Commun.* **60**, 1384-1390.

Birkett, C. R., Foster, K. E. and Gull, K. (1985). Evolution and patterns of expression of the *Physarum* multi-tubulin family analysed by the use of monoclonal antibodies. In *Molecular Genetics of Filamentous Fungi*, pp. 265-275. Alan R. Liss, New York.

Blose, S. H., Melzer, D. I. and Feramisco, J. R. (1984). 10-nm filaments are induced to collapse in living cells microinjected with monoclonal and polyclonal antibodies against tubulin. *J. Cell Biol.* **98**, 847-858.

Bré, M. H., de Néchaud, B., Wolff, A. and Fleury, A. (1994). Glutamylated tubulin probed in ciliates with the monoclonal antibody GT335. *Cell Motil. Cytoskel.* **27**, 337-349.

Breitling, F. and Little, M. (1986). Carboxy-terminal regions on the surface of tubulin and microtubules. Epitope locations of YOL 1/34, DM1A and DM1B. *J. Mol. Biol.* **189**, 367-370.

Brown, H. R. and Erickson, H. P. (1983). Assembly of proteolytically cleaved tubulin. *Arch. Biochem. Biophys.* **220**, 46-51.

Brugerolle, G. and Adoutte, A. (1988). Probing protistan phylogenies with an anti-tubulin antibody. *BioSystems* **21**, 255-268.

Callen, A. M., Adoutte, A., Andreu, J. M., Baroin-Tourancheau, A., Bré, M. H., Calvo Ruiz, P., Clérot, J. C., Delgado, P., Fleury, A., Jeanmaire-Wolf, R., Viklicky, V., Villalobo, E. and Levilliers, N. (1994). Isolation and characterization of libraries of monoclonal antibodies directed against various forms of tubulin in *Paramecium*. *Biol. Cell* **81**, 95-119.

Canas, B., Dai, Z., Lackland, H., Poretz, R. and Stein, S. (1993). Covalent attachment of peptides to membranes for dot-blot analysis of glycosylation sites and epitopes. *Anal. Biochem.* **211**, 179-182.

Cleveland, D. W., Fischer, S. G., Kirschner, M. W. and Laemmli, U. K. (1977). Peptide mapping by limited proteolysis in sodium dodecyl sulfate and analysis by gel electrophoresis. *J. Biol. Chem.* **252**, 1102-1106.

Cleveland, D. W. and Sullivan, K. F. (1985). Molecular biology and genetics of tubulin. *Annu. Rev. Biochem.* **54**, 331-365.

Cohen, J., Adoutte, A., Grandchamp, S., Houdebine, L. M. and Beisson, J. (1982). Immunocytochemical study of microtubular structures throughout the cell cycle of *Paramecium*. *Biol. Cell* **44**, 35-44.

Cohen, J. and Beisson, J. (1988). The cytoskeleton. In *Paramecium*. (ed. H.-D. Görtz), pp. 363-392. Springer-Verlag, Berlin, Heidelberg.

de la Vina, S., Andreu, D., Medrano, F. J., Nieto, J. M. and Andreu, J. M. (1988). Tubulin structure probed with antibodies to synthetic peptides. Mapping of three major types of limited proteolysis fragments. *Biochemistry* **27**, 5352-5365.

Denoulet, P., Eddé, B., Pinto-Henrique, D., Koulakoff, A., Berwald-Netter Y. and Gros, F. (1988). The increase of tubulin heterogeneity during differentiation of neurons in primary culture is controlled mainly at the post-translational level. In *Structure and Functions of the Cytoskeleton*, vol. 171 (ed. B. A. F. Rousset), pp. 231-237. Colloque INSERM/John Libbey Eurotext Ltd, London, Paris.

Diaz-Nido, J., Serrano, L., Lopez-Otin, C., Vandekerckhove, J. and Avila, J. (1990). Phosphorylation of a neuronal-specific β-tubulin isotype. *J. Biol. Chem.* **265**, 13949-13954.

Dupuis, P. (1992a). Structure, Organisation et Expression des Gènes de Tubuline chez la Paramécie. Doctoral thesis, Université Paris XI, Orsay.

Dupuis, P. (1992b). The beta-tubulin genes of *Paramecium* are interrupted by two 27 bp introns. *EMBO J.* **11**, 3713-3719.

Eddé, B., Rossier, J., Le Caer, J. P., Desbruyères, E., Gros, F. and Denoulet, P. (1990). Posttranslational glutamylation of α-tubulin. *Science* **247**, 83-85.

Eddé, B., Rossier, J., Le Caer, J. P., Berwald-Netter, Y., Koulakoff, A., Gros, F. and Denoulet, P. (1991). A combination of posttranslational modifications is responsible for the production of neuronal α-tubulin heterogeneity. *J. Cell. Biochem.* **46**, 134-142.

Eipper, B. A. (1974). Properties of rat brain tubulin. *J. Biol. Chem.* **249**, 1407-1416.

Fleury, A., Callen, A. M., Bré, M. H., Iftode, F., Jeanmaire-Wolf, R., Levilliers, N. and Clérot, J. C. (1995). Where and when is microtubule diversity generated in *Paramecium*? Immunological properties of microtubular networks in the interphase and dividing cells. *Protoplasma* (in press).

Fouquet, J. P., Eddé, B., Kann, M. L., Wolff, A., Desbruyères, E. and Denoulet, P. (1994). Differential distribution of glutamylated tubulin during spermatogenesis in mammalian testis. *Cell Motil. Cytoskel.* **27**, 49-58.

Gaertig, J., Thatcher, T. H., McGrath, K. E., Callahan, R. C. and Gorovsky, M. A. (1993). Perspectives on tubulin isotype function and evolution based on the observation that *Tetrahymena thermophila* microtubules contain a single α- and β-tubulin. *Cell Motil. Cytoskel.* **25**, 243-253.

Gaunitz, F. (1990). Charakterisierung von α-Tubulingenen aus den Makronuclei verschiedener hypotricher Ciliaten. Doctoral thesis, Eberhard-Karls-Universität, Tübingen.

Gelfand, V. I. and Bershadsky, A. D. (1991). Microtubule dynamics: mechanism, regulation, and function. *Annu. Rev. Cell Biol.* **7**, 93-116.

Geuens, G., Hill, A. M., Levilliers, N., Adoutte, A. and DeBrabander, M. (1989). Microtubule dynamics investigated by microinjection of *Paramecium* axonemal tubulin: lack of nucleation but proximal assembly of microtubules at the kinetochore during prometaphase. *J. Cell Biol.* **108**, 939-953.

Gibbons, I. R. and Fronk, E. (1972). Some properties of bound and soluble dynein from sea urchin sperm flagella. *J. Cell Biol.* **54**, 365-381.

Greer, K. and Rosenbaum J. L. (1989). Post-translational modifications of tubulin. In *Cell Movement*, vol. 2, *Kinesin, Dynein and Microtubule Dynamics* (ed. F. D. Warner and J. R. McIntosh), pp. 47-66. Alan R. Liss, New York.

Grimm, M., Breitling, F. and Little, M. (1987). Location of the epitope for the α-tubulin monoclonal antibody TU-01. *Biochim. Biophys. Acta* **914**, 83-88.

Gu, W., Lewis, S. A. and Cowan, N. J. (1988). Generation of antisera that discriminate among mammalian α-tubulins: introduction of specialized isotypes into cultured cells results in their coassembly without disruption of normal microtubule function. *J. Cell Biol.* **106**, 2011-2022.

Gundersen, G. G. and Bulinski, J. C. (1986). Microtubule arrays in differentiated cells contain elevated levels of a post-translationally modified form of tubulin. *Eur. J. Cell Biol.* **42**, 288-294.

Helftenbein, E. and Müller, E. (1988). Both α-tubulin genes are transcriptionally active in *Stylonychia lemnae*. *Curr. Genet.* **13**, 425-432.

Hirano-Ohnishi, J. and Watanabe Y. (1989). Ca^{2+}/calmodulin-dependent phosphorylation of ciliary β-tubulin in *Tetrahymena*. *J. Biochem.* **105**, 858-860.

Iftode, F., Cohen, J., Ruiz, F., Torres Rueda, A., Chen-Shan, L., Adoutte, A. and Beisson, J. (1989). Development of surface pattern during division in *Paramecium*. I. Mapping of duplication and reorganization of cortical cytoskeletal structures in the wild type. *Development* **105**, 191-211.

Joshi, H. C. and Cleveland, D. W. (1990). Diversity among tubulin subunits: toward what functional end? *Cell Motil. Cytoskel.* **16**, 159-163.

Kilmartin, J. V., Wright, B. and Milstein, C. (1982). Rat monoclonal antitubulin antibodies derived by using a new nonsecreting rat cell line. *J. Cell Biol.* **93**, 576-582.

Krauhs, E., Little, M., Kempf, T., Hofer-Warbinek, R., Ade, W. and Ponstingl, H. (1981). Complete amino acid sequence of β-tubulin from porcine brain. *Proc. Nat. Acad. Sci. USA* **78**, 4156-4160.

Kyhse-Andersen, J. (1984). Electroblotting of multiple gels: a simple apparatus without buffer tank for rapid transfer of proteins from polyacrylamide to nitrocellulose. *J. Biochem. Biophys. Meth.* **10**, 203-209.

Laemmli, U. K. (1970). Cleavage of structural proteins during the assembly of the head of bacteriophage T4. *Nature* **277**, 680-685.

LeDizet, M. and Piperno, G. (1987). Identification of an acetylation site of *Chlamydomonas* α-tubulin. *Proc. Nat. Acad. Sci. USA* **84**, 5720-5724.

LeDizet, M. and Piperno, G. (1991). Detection of acetylated α-tubulin by specific antibodies. *Meth. Enzymol.* **196**, 264-274.

L'Hernault, S. W. and Rosenbaum, J. L. (1983). *Chlamydomonas* α-tubulin is posttranslationally modified in the flagella during flagellar assembly. *J. Cell Biol.* **97**, 258-263.

L'Hernault, S. W. and Rosenbaum, J. L. (1985). *Chlamydomonas* α-tubulin is posttranslationally modified by acetylation on the ε-amino group of a lysine. *Biochemistry* **24**, 473-478.

Liang, A. and Heckmann, K. (1993). *Blepharisma* uses UAA as a termination codon. *Naturwissenschaften* **80**, 225-226.

Liang, A., Schmidt, H. J. and Heckmann, K. (1994). The alpha and beta tubulin genes of *Euplotes octocarinatus*. *J. Euk. Microbiol.* **41**, 163-169.

Little, M., Luduena, R. F., Langford, G. M., Asnes C. F. and Farrell, K. (1981). Comparison of proteolytic cleavage patterns of α-tubulins and β-tubulins from taxonomically distant species. *J. Mol. Biol.* **149**, 95-107.

Little, M., Luduena, R. F., Keenan, R. and Asnes, C. F. (1982). Tubulin evolution: two major types of α-tubulin. *J. Mol. Evol.* **19**, 80-86.

Little, M., Luduena, R. F., Morejohn, L. C., Asnes, C. and Hoffman, E. (1984a). The tubulins of animals, plants, fungi and protists: implications for metazoan evolution. *Origins of Life* **13**, 169-176.

Little, M., Luduena, R. F., Quinlan, R. A., Ponstingl, H., Krauhs, E. and Raff, E. C. (1984b). Some aspects of tubulin structure and tissue specificity. *J. Submicrosc. Cytol.* **16**, 11-13.

Little, M. and Seehaus, T. (1988) Comparative analysis of tubulin sequences. *Comp. Biochem. Physiol* **90B**, 655-670.

Lobert, S., Hennington, B. S. and Correia, J. J. (1993). Multiple sites for subtilisin cleavage of tubulin: effects of divalent cations. *Cell Motil. Cytoskel.* **25**, 282-297.

Luduena, R. F. (1993). Are tubulin isotypes functionally significant. *Mol. Biol. Cell* **4**, 445-457.

Luduena, R. F., Zimmermann, H. P. and Little, M. (1988). Identification of the phosphorylated β-tubulin isotype in differentiated neuroblastoma cells. *FEBS Lett.* **230**, 142-146.

Maccioni, R. B., Serrano, L., Avila, J. and Cann J. R. (1986). Characterization and structural aspects of the enhanced assembly of tubulin after removal of its carboxyl-terminal domain. *Eur. J. Biochem.* **156**, 375-381.

McGrath, K. E., Yu, S. M., Heruth, D. P., Kelly, A. A. and Gorovsky, M. A.

(1994). Regulation and evolution of the single alpha-tubulin gene of the ciliate *Tetrahymena thermophila*. *Cell Motil. Cytoskel.* **27**, 272-283.

McKeithan, T. W., Lefebvre, P. A., Silflow, C. and Rosenbaum, J. L. (1983). Multiple forms of tubulin in *Polytomella* and *Chlamydomonas*: evidence for a precursor of flagellar α-tubulin. *J. Cell Biol.* **96**, 1056-1063.

Mandelkow, E. M., Herrmann, M. and Rühl, R. (1985). Tubulin domains probed by limited proteolysis and subunit-specific antibodies. *J. Mol. Biol.* **185**, 311-327.

Mary, J., Redeker, V., Le Caer, J. P., Promé, J. C. and Rossier, J. (1994). Class I and IVa β-tubulin isotypes expressed in adult mouse brain are glutamylated. *FEBS Lett.* **353**, 89-94.

Matten, W. T., Aubry, M., West, J. and Maness, P. F. (1990). Tubulin is phosphorylated at tyrosine by $pp60^{c\text{-}src}$ in nerve growth cone membranes. *J. Cell Biol.* **111**, 1959-1970.

Merril, C. R., Goldman, D., Sedman, S. A. and Ebert, M. H. (1981). Ultrasensitive stain for proteins in polyacrylamide gels shows regional variation in cerebrospinal fluid proteins. *Science* **211**, 1437-1438.

Merril, C. R., Goldman, D. and Van Keuren, M. L. (1983). Silver staining methods for polyacrylamide gel electrophoresis. *Meth. Enzymol.* **96**, 230-239.

Paschal, B. M., Obar, R. A. and Vallee R. B. (1989). Interaction of brain cytoplasmic dynein and MAP2 with a common sequence at the C terminus of tubulin. *Nature* **342**, 569-572.

Paturle-Lafanechère, L., Eddé, B., Denoulet, P., Van Dorsselaer, A., Mazarguil, H., Le Caer, J. P., Wehland, J. and Job, D. (1991): Characterization of a major brain tubulin variant which cannot be tyrosinated. *Biochemistry* **30**, 10523-10528.

Paturle-Lafanechère, L., Manier, M., Trigault, N., Pirollet, F., Mazarguil, H. and Job, D. (1994). Accumulation of delta 2-tubulin, a major tubulin variant that cannot be tyrosinated, in neuronal tissues and in stable microtubule assemblies. *J. Cell Sci.* **107**, 1529-1543.

Piperno, G. and Fuller, M. T. (1985): Monoclonal antibodies specific for an acetylated form of α-tubulin recognize the antigen in cilia and flagella from a variety of organisms. *J. Cell Biol.* **101**, 2085-2094.

Raff, E. C. (1984). Genetics of microtubule systems. *J. Cell Biol.* **99**, 1-10.

Redeker, V., Melki, R., Promé, D., Le Caer, J. P. and Rossier, J. (1992). Structure of tubulin C-terminal domain obtained by subtilisin treatment. The major α and β tubulin isotypes from pig brain are glutamylated. *FEBS Lett.* **313**, 185-192.

Redeker, V., Levilliers, N., Schmitter, J. M., Le Caer, J. P., Rossier, J., Adoutte, A. and Bré, M. H. (1994). Polyglycylation of tubulin: a posttranslational modification in axonemal microtubules. *Science* **266**, 1688-1691.

Renthal, R., Schneider, B. G., Miller, M. M. and Luduena, R. F. (1993). β_{IV} is the major β-tubulin isotype in bovine cilia. *Cell Motil. Cytoskel.* **25**, 19-29.

Rüdiger, M., Plessman, U., Klöppel, K. D., Wehland, J. and Weber, K. (1992). Class II tubulin, the major brain β tubulin isotype is polyglutamylated on glutamic acid residue 435. *FEBS Lett.* **308**, 101-105.

Rüdiger, M. and Weber, K. (1993). Characterization of the post-translational modifications in tubulin from the marginal band of avian erythrocytes. *Eur. J. Biochem.* **218**, 107-116.

Rüdiger, M., Wehland, J. and Weber, K. (1994). The carboxy-terminal peptide of detyrosinated α tubulin provides a minimal system to study the substrate specificity of tubulin-tyrosine ligase. *Eur. J. Biochem.* **220**, 309-320.

Russell, D. G. and Gull, K. (1984). Flagellar regeneration of the trypanosome *Crithidia fasciculata* involves post-translational modification of cytoplasmic alpha tubulin. *Mol. Cell. Biol.* **4**, 1182-1185.

Russell, D. G., Miller, D. and Gull, K. (1984). Tubulin heterogeneity in the trypanosome *Crithidia fasciculata*. *Mol. Cell. Biol.* **4**, 779-790.

Sackett, D. L., Bhattacharyya, B. and Wolff, J. (1985). Tubulin subunit carboxyl termini determine polymerization efficiency. *J. Biol. Chem.* **260**, 43-45.

Serrano, L., Avila, J. and Maccioni, R. B. (1984a). Controlled proteolysis of tubulin by subtilisin: localization of the site for MAP_2 interaction. *Biochemistry* **23**, 4675-4681.

Serrano, L., de la Torre, J., Maccioni, R. B. and Avila, J. (1984b). Involvement of the carboxyl-terminal domain of tubulin in the regulation of its assembly. *Proc. Nat. Acad. Sci. USA* **81**, 5989-5993.

Serrano, L., Wandosell, F., de la Torre, J. and Avila, J. (1986). Proteolytic modification of tubulin. *Meth. Enzymol.* **134**, 179-190.

Silflow, C. D. (1991). Why do tubulin gene families lack diversity in flagellate/ciliate protists? *Protoplasma* **164**, 9-11.

Sonderegger, P., Jaussi, R., Gehring, H., Brunschweiler, K. and Christen, P. (1982). Peptide mapping of protein bands from polyacrylamide gel electrophoresis by chemical cleavage in gel pieces and re-electrophoresis. *Anal. Biochem.* **122**, 298-301.

Stieger, J., Wyler, T. and Seebeck, T. (1984). Partial purification and characterization of microtubular protein from *Trypanosoma brucei*. *J. Biol. Chem.* **259**, 4596-4602.

Sullivan, K. F. (1988). Structure and utilization of tubulin isotypes. *Annu. Rev. Cell Biol.* **4**, 687-716.

Suprenant, K. A., Hays, E., LeCluyse, E. and Dentler, W. L. (1985). Multiple forms of tubulin in the cilia and cytoplasm of *Tetrahymena thermophila*. *Proc. Nat. Acad. Sci. USA* **82**, 6908-6912.

Thompson, W. C. (1982). The cyclic tyrosination/detyrosination of alpha tubulin. *Meth. Cell Biol.* **24**, 235-255.

Torres, A. and Delgado, P. (1989). Effects of cold and nocodazole treatments on the microtubular systems of *Paramecium* in interphase. *J. Protozool.* **36**, 113-119.

Towbin, H., Staehelin, T. and Gordon, J. (1979). Electrophoretic transfer of proteins from polyacrylamide gels to nitrocellulose sheets: procedure and some applications. *Proc. Nat. Acad. Sci. USA* **76**, 4350-4354.

Viklicky, V., Draber, P., Hasek, J. and Bartek, J. (1982). Production and characterization of a monoclonal antitubulin antibody. *Cell Biol. Int. Rep.* **6**, 725-731.

Wehland, J., Schröder, H. C. and Weber, K. (1984). Amino acid sequence requirements in the epitope recognized by the α-tubulin-specific rat monoclonal antibody YL 1/2. *EMBO J.* **3**, 1295-1300.

Wolff, A., de Néchaud, B., Chillet, D., Mazarguil, H., Desbruyères, E., Audebert, S., Eddé, B., Gros, F. and Denoulet, P. (1992). Distribution of glutamylated α and β-tubulin in mouse tissues using a specific monoclonal antibody, GT335. *Eur. J. Cell Biol.* **59**, 425-432.

(Received 3 January 1995 - Accepted 1 June 1995)